

Normal random matrix ensemble as a growth problem

R. Teodorescu ^{a,1}, E. Bettelheim ^{b,2}, O. Agam ^b, A. Zabrodin ^c,
and P. Wiegmann ^d

^a*James Frank Institute, University of Chicago, 5640 S. Ellis Ave. Chicago, IL 60637, USA.*

^b*Racah Institute of Physics, Hebrew University, Givat Ram, Jerusalem, Israel 91904*

^c*Institute of Biochemical Physics, Kosygina str. 4, 117334 Moscow, Russia also at ITEP, Bol. Chermushkinskaya str. 25, 117259 Moscow, Russia*

^d*James Frank Institute, Enrico Fermi Institute, University of Chicago, 5640 S. Ellis Ave. Chicago, IL and the Landau Institute, Moscow, Russia*

Abstract

In general or normal random matrix ensembles, the support of eigenvalues of large size matrices is a planar domain (or several domains) with a sharp boundary. This domain evolves under a change of parameters of the potential and of the size of matrices. The boundary of the support of eigenvalues is a real section of a complex curve. Algebraic-geometrical properties of this curve encode physical properties of random matrix ensembles. This curve can be treated as a limit of a spectral curve which is canonically defined for models of finite matrices. We interpret the evolution of the eigenvalue distribution as a growth problem, and describe the growth in terms of evolution of the spectral curve. We discuss algebraic-geometrical properties of the spectral curve and describe the wave functions (normalized characteristic polynomials) in terms of differentials on the curve. General formulae and emergence of the spectral curve are illustrated by three meaningful examples.

Key words: Integrable Systems, Random Matrix Theory, Stochastic Growth
PACS: 02.50.Ey, 02.30.-f

Email addresses: rteodore@uchicago.edu (R. Teodorescu),
eldadb@phys.huji.ac.il (E. Bettelheim), zabrodin@itep.ru (A. Zabrodin),
wiegmann@uchicago.edu (P. Wiegmann).

¹ Present address: Physics Department, Columbia University, New York.

² Present address: James Frank Institute, University of Chicago, 5640 S. Ellis Ave. Chicago, IL 60637, USA.

1 Introduction and Preliminaries

Recently, random matrix theory has found new applications in growth problems, where the evolution of the interface separating domains of different nature is a subject of interest. In some realizations, the growing domain is an aggregate of randomly deposited subunits.

In general random matrix ensembles, complex eigenvalues usually occupy planar domains in the complex plane. Their boundaries become sharp as the size of matrices, N , goes to infinity. It appears that, for an important class of growth models, the aggregates evolve similarly to the support of eigenvalues of general matrix ensembles. In Refs. [1,2,3], one of the most interesting classes of growth problems – Laplacian growth – has been linked to the evolution of normal random matrices.

The interpretation of random matrix theory in terms of an aggregation process seems to be a productive approach in a number of different applications. Among them are the growth problems mentioned above, the semiclassical behavior of electronic droplets in the Quantum Hall regime [2], and $\mathcal{N} = 1$ supersymmetric Yang-Mills theory [4]. They reveal a relatively new, geometrical aspect of random matrix theory. From the mathematical point of view, the connection of random matrix ensembles with isomonodromic deformations of differential equations [5,6,7,8] seems to be especially interesting for these applications.

It has been emphasized in recent papers [4] and [9] that the boundary of the domains of eigenvalues is to be thought of as a real section of a complex algebraic curve (a Riemann surface). This curve appears to be a fundamental object of random matrix theory. It encodes the most interesting physical properties of matrix ensembles (see, e.g., [4,9,10,11] for the complex curves in one- and two-matrix models).

In the Hermitian or unitary ensembles, the support of eigenvalues is a set of line intervals. Their boundaries are just points. In general matrix ensembles, eigenvalues are complex numbers, and their support is a planar domain. The boundaries are planar curves, evolving in a complicated and unstable manner. The notion of complex curve naturally links the planar geometry of the boundaries to the algebro-geometric properties of the matrix ensemble.

In this paper we present general aspects of the normal matrix ensemble from this standpoint. One may canonically associate a complex curve to the matrix ensemble, not only in the large N limit, but for any finite N as well. It is the spectral curve of the operator which generates recursion relations (the Lax operator), projected to a certain finite-dimensional subspace. In the large N limit (a semiclassical limit), this curve becomes the complex curve which

describes the support of eigenvalues.

We introduce the spectral curve for normal matrix ensembles, and describe the evolution of the curve with respect to parameters of the statistical weight of the ensemble (*deformation parameters*) and the size of matrices (a parameter of *growth*). In a forthcoming paper, we will prove that the semiclassical limit of the evolution (or deformation) equations is the universal Whitham hierarchy associated with the complex curve. The semiclassical wave function can be expressed through differentials on the curve. We also notice that the Whitham hierarchy is identical to the set of equations which describe Laplacian growth processes – unstable dynamics of an interface between two immiscible phases.

Three meaningful examples illustrate the general formulae.

1.1 Normal matrix ensemble

A matrix M is called normal if it commutes with its Hermitian conjugate: $[M, M^\dagger] = 0$, so that both M and M^\dagger can be diagonalized simultaneously. Eigenvalues of normal matrices are complex. The statistical weight of the normal matrix ensemble is given through a general potential $W(M, M^\dagger)$ [12]:

$$e^{\frac{1}{\hbar} \text{tr} W(M, M^\dagger)} d\mu(M). \quad (1)$$

Here \hbar is a parameter, and the measure of integration over normal matrices is induced by the flat metric on the space of all complex matrices $d_C M$, where $d_C M = \prod_{ij} d \text{Re} M_{ij} d \text{Im} M_{ij}$. Using the standard procedure, (see, e.g., [13]) one passes to the joint probability distribution of eigenvalues of normal matrices z_1, \dots, z_N , where N is size of the matrix:

$$\frac{1}{N! \tau_N} |\Delta_N(z)|^2 \prod_{j=1}^N e^{\frac{1}{\hbar} W(z_j, \bar{z}_j)} d^2 z_j \quad (2)$$

Here $d^2 z_j \equiv dx_j dy_j$ for $z_j = x_j + iy_j$, $\Delta_N(z) = \det(z_j^{i-1})_{1 \leq i, j \leq N} = \prod_{i>j}^N (z_i - z_j)$ is the Vandermonde determinant, and

$$\tau_N = \frac{1}{N!} \int |\Delta_N(z)|^2 \prod_{j=1}^N e^{\frac{1}{\hbar} W(z_j, \bar{z}_j)} d^2 z_j \quad (3)$$

is the normalization factor. This is the partition function of the matrix model (a τ -function).

A particularly important special case arises if the potential W has the form

$$W = -|z|^2 + V(z) + \overline{V(z)}, \quad (4)$$

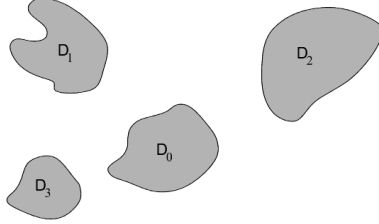


Fig. 1. A support of eigenvalues consisting of four disconnected components.



Fig. 2. The distribution of eigenvalues for the Gaussian potential. The droplet is an ellipse with quadrupole moment $2|t_2|$ and area $\pi\hbar N$.

where $V(z)$ is a holomorphic function in a domain which includes the support of eigenvalues (see also a comment in the end of Sec. 1.6 about a proper definition of the ensemble with this potential). In this case, a normal matrix ensemble gives the same distribution as a general complex matrix ensemble. A general complex matrix can be decomposed as $M = U(Z + R)U^\dagger$, where U and Z are unitary and diagonal matrices, respectively, and R is an upper triangular matrix. The distribution (2) holds for the elements of the diagonal matrix Z which are eigenvalues of M (Ref. [13]). Here we mostly focus on the special potential (4), and also assume that the field

$$A(z) = \partial_z V(z) \quad (5)$$

(a “vector potential”, see Sec. 1.5) is a globally defined meromorphic function.

1.2 Droplets of eigenvalues

In a proper large N limit ($\hbar \rightarrow 0$, $N\hbar$ fixed), the eigenvalues of matrices from the ensemble densely occupy a connected domain D in the complex plane, or, in general, several disconnected domains. This set (called the support of eigenvalues) has sharp edges (Fig. 1). We refer to the connected components D_α of the domain D as *droplets*.

In the case of algebraic domains (the definition follows) the eigenvalues are distributed with the density $\rho = -\frac{1}{4\pi}\Delta W$, where $\Delta = 4\partial_z\partial_{\bar{z}}$ is the 2-D Laplace operator [14]. For the potential (4) the density is uniform. The shape of the support of eigenvalues is a more involved subject. We discuss it below. For example, if the potential is Gaussian [15],

$$A(z) = 2t_2z, \quad (6)$$

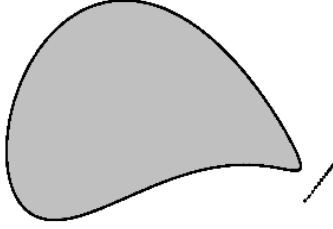


Fig. 3. The distribution of eigenvalues for the potential $V(z) = -\alpha \log(1 - z/\beta) - \gamma z$. If the area of the droplet is $\pi\hbar N$, the complement of the droplet is an algebraic domain which can be conformally mapped to the exterior of the unit disk by the Joukowski map (61). In this case, the cut of the Schwarz function shown in the figure (corresponding to a virtual droplet located on the unphysical sheet) shrinks to a double point.

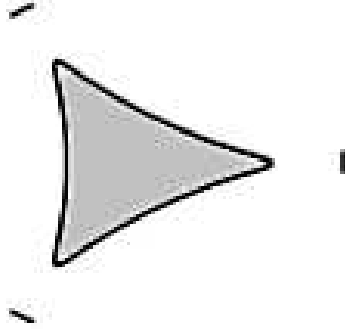


Fig. 4. The distribution of eigenvalues for the potential $V(z) = t_3 z^3$. Cuts of the Schwarz function are shown. The cuts correspond to virtual droplets located on unphysical sheets. If the area of the droplet is $\pi\hbar N$, the cuts shrink to double points. The boundary contour is a hypotrochoid.

the domain is an ellipse (see Fig. 2). If A has one simple pole,

$$A(z) = -\frac{\alpha}{z - \beta} - \gamma \quad (7)$$

the droplet (under certain conditions discussed below) has the profile of an aircraft wing given by the Joukowski map (Fig. 3). If A has one double pole (say, at infinity),

$$A(z) = 3t_3 z^3, \quad (8)$$

the droplet is a hypotrochoid (Fig. 4). These are the three examples that we will discuss below in detail. If A has two or more simple poles, there may be more than one droplet.

If $A(z)$ is a more complicated function, the domain of eigenvalues develops an unstable fingering pattern, similar to the one in Fig. 5.

Boundary components of the droplets form a real section of a complex curve.



Fig. 5. A grown fingering pattern observed in a radial Hele-Shaw cell. Air is inserted under pressure to the cell filled by silicon oil [16].

1.3 Semiclassical complex curve

Jumping ahead, we describe the construction of the semiclassical complex curve which emerges in the normal matrix ensemble. Let us represent the boundary of the domain as a real curve $F(x, y) = 0$. If the vector potential $A(z)$ is a meromorphic function (we always assume that this is the case), the function F can be chosen to be an irreducible polynomial. Then we rewrite it in holomorphic coordinates as

$$F\left(\frac{z + \bar{z}}{2}, \frac{z - \bar{z}}{2i}\right) = f(z, \bar{z}) \quad (9)$$

and treat z and \bar{z} as independent complex coordinates z, \tilde{z} . The equation $f(z, \tilde{z}) = 0$ defines a complex curve. This curve is a finite-sheet covering of the z -plane. The single-valued function $\tilde{z}(z)$ on the curve is a multivalued function on the z -plane. Making cuts, one can fix single-valued branches of this function.

The boundary of the domain is a section of the curve by the plane where \tilde{z} is complex conjugate of z . It belongs to a particular sheet (we call it the *physical sheet*) of the covering. It appears that physical properties of the ensemble are determined not only by the physical sheet, but rather by the entire algebraic covering, including all the sheets other than physical. The Riemann surface for Example (7) is presented in Fig. 10.

1.4 Growth and deformation parameters. Evolution of the curve

Similarly to the Hermitian matrix ensemble [4,9,10,11], the complex curve of the normal matrix ensemble is characterized by the potential W , or by the “vector potential” $A(z)$, and by a set of $g + 1$ integers ν_α (not necessarily positive), where g is genus of the curve. The integers are subject to the constraint

$\sum_{\alpha=0}^g \nu_{\alpha} = N$. We will discuss the meaning of these numbers later on. For now, we only mention that if they are all positive, then they are proportional to the areas of the droplets of uniformly distributed eigenvalues. Every droplet contains ν_{α} eigenvalues, so a quantum of area is $\pi\hbar$ per particle.

As one varies the potential and the filling factors ν_{α} , the curve and the interface bounding the droplets evolve. Parameters of the potential (for example, poles and residues of the meromorphic function (5)) and filling numbers are *deformation parameters* and *parameters of growth*. They are coordinates in the moduli space of the complex curves.

An infinitesimal variation of the potential generates correlation functions of the ensemble (Ref. [14]). For example, irreducible correlation functions of resolvents (holomorphic currents) $J(z) = \text{tr} \frac{\hbar}{z-M} = \sum_i \frac{\hbar}{z-z_i}$ are generated by variations of $A(z)$. In Ref. [14] we showed that the correlation functions are expressed through algebro-geometrical properties of the boundary of the domain.

During the evolution, the genus of the complex curve may change. This corresponds to a coalescence of droplets or a droplet breakup, or even more complicated degenerations, when a droplet shrinks to a point and simultaneously merges with another droplet. Close to degeneracy points (also called critical points), matrix ensembles have universal scaling behavior. We will present a study of this problem in a future paper.

A particularly interesting process is *growth*. In this case, one changes the total number of eigenvalues N and keeps the potential fixed. Below we refer to the normalized total number of particles

$$t = \hbar N$$

as *time of growth*. In the algebraic case, the time t is the normalized (modulo π) area of the droplets. While N increases, the new eigenvalues aggregate at the boundary of the existing droplets, so that the domain of eigenvalues (an aggregate) grows (Fig. 6). Growth of a hypotrochoid is depicted in Fig. 7.

There are several important physical problems where this kind of evolution occurs. We list them in historical order.

The first one is the celebrated Hele-Shaw problem – the most studied example of Laplacian growth. The Hele-Shaw problem describes the non-equilibrium dynamics of a planar interface between two immiscible fluids confined to a thin 2-D cell. The second one is the matrix model description of 2-D quantum gravity. The third one is the evolution of energy levels in mesoscopic systems. A similar problem also emerges in isomonodromic deformation of differential equations.

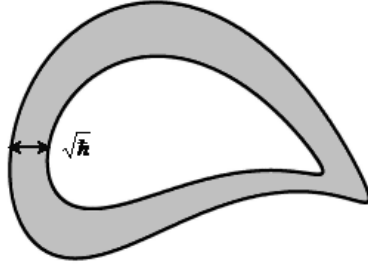


Fig. 6. The area of a droplet grows with the rate $\pi\hbar$ per eigenvalue. A new eigenvalue aggregates at the boundary of the droplet. The shaded area depicts the support of the semiclassical wave function.

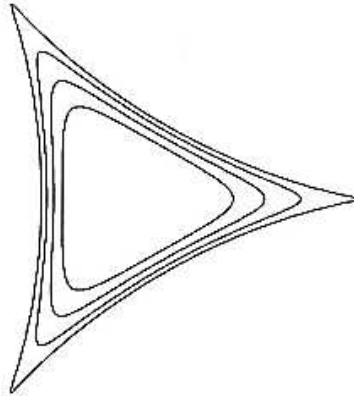


Fig. 7. Hypotrochoid grows until it reaches a critical point.

The last three problems and their connection with the matrix ensemble are well reflected in the literature (see e.g., [7,8,17] for reviews). The connection of matrix ensembles to the Hele-Shaw problem is relatively new. It nicely illustrates the growth and gives a transparent hydrodynamic interpretation to abstract objects of algebraic geometry of curves and complex analysis on Riemann surfaces. We find that a brief description of the Hele-Shaw problem in this paper is in order (see Sec. 7).

1.5 Normal matrix ensemble and quantum Hall effect

A useful interpretation of the Coulomb gas distribution (2) is a coherent state of relativistic electrons in the Quantum Hall regime [2]. In this case, the electrons are situated in the plane in a strong, not necessarily uniform, magnetic field $B(z) = -\frac{1}{2}\Delta W$, and fully occupy the lowest energy level. The exact N -particle wave function, defined up to a phase, is

$$\Psi_N(z_1, \dots, z_N) = \frac{1}{\sqrt{N!\tau_N}} \Delta_N(z) e^{\sum_{j=1}^N \frac{1}{2\hbar} W(z_j, \bar{z}_j)}. \quad (10)$$

The joint probability distribution (2) is then equal to $|\Psi(z_1, \dots, z_N)|^2$. It is the probability to find electrons at the points z_i . In the semiclassical regime, the wave function (10) describes an incompressible electronic droplet with sharp edges. The function $A(z)$ (5) can be thought of as a holomorphic component of the vector potential generated by magnetic impurities located far away from the electronic droplet.

In this language, the growth problem translates into the evolution of a semi-classical electronic droplet under a change of magnetic field or chemical potential.

1.6 Orthogonal polynomials as a measure of growth

Let the number of eigenvalues (particles) increase while the potential stays fixed. If the support of eigenvalues is simply-connected, its area grows as $\hbar N$. One can describe the evolution of the domain through the density of particles

$$\rho_N(z) = N \int |\Psi_N(z, z_1, z_2, \dots, z_{N-1})|^2 d^2 z_1 \dots d^2 z_{N-1}, \quad (11)$$

where Ψ_N is given by (10).

We introduce a set of orthonormal one-particle functions on the complex plane as matrix elements of transitions between N and $(N+1)$ -particle states:

$$\frac{\psi_N(z)}{\sqrt{N+1}} = \int \Psi_{N+1}(z, z_1, z_2, \dots, z_N) \overline{\Psi_N(z_1, z_2, \dots, z_N)} d^2 z_1 \dots d^2 z_N \quad (12)$$

Then the rate of the density change is

$$\rho_{N+1}(z) - \rho_N(z) = |\psi_N(z)|^2. \quad (13)$$

The proof of this formula is based on the representation of the ψ_n through holomorphic biorthogonal polynomials $P_n(z)$. Up to a phase

$$\psi_n(z) = e^{\frac{1}{2\hbar}W(z, \bar{z})} P_n(z), \quad P_n(z) = \sqrt{\frac{\tau_n}{\tau_{n+1}}} z^n + \dots \quad (14)$$

The polynomials $P_n(z)$ are biorthogonal on the complex plane with the weight $e^{W/\hbar}$:

$$\int e^{W/\hbar} P_n(z) \overline{P_m(z)} d^2 z = \delta_{mn}. \quad (15)$$

The proof of these formulae is standard in the theory of orthogonal polynomials. Extension to the biorthogonal case adds no difficulties.

A physical interpretation of the wave function ψ_n is clear in the QHE setup. The eigenvalues z_i are the positions of electrons in a strong magnetic field.

Then $|\psi_N(z)|^2$ is a probability of adding an additional electron to an aggregate of N electrons at the point z . Since the droplet is incompressible, it is only possible to add the particle to the boundary of the droplet. We will see that the wave function in a semiclassical limit is indeed localized on the boundary.

We note that, with the choice of potential (4), the integral representation (15) has only a formal meaning, since the integral diverges unless the potential is Gaussian. A proper definition of the wave functions goes through recursive relations (17, 18) which follow from the integral representation. The same comment applies to the τ -function (3). The wave function is not normalized everywhere in the complex plane. It may diverge at the poles of the vector potential field.

Below we describe the evolution and semiclassical behavior of the wave function in the region of the complex plane close to the boundary of physical droplets.

2 Equations for the wave functions and the spectral curve

In this section we specify the potential to be of the form (4). It is convenient to modify the exponential factor of the wave function. Namely, we define

$$\psi_n(z) = e^{-\frac{|z|^2}{2\hbar} + \frac{1}{\hbar}V(z)}P_n(z), \quad \text{and} \quad \chi_n(z) = e^{\frac{1}{\hbar}V(z)}P_n(z), \quad (16)$$

where the holomorphic functions $\chi_n(z)$ are orthonormal in the complex plane with the weight $e^{-|z|^2/\hbar}$. Like traditional orthogonal polynomials, the biorthogonal polynomials P_n (and the corresponding wave functions) obey a set of differential equations with respect to the argument z , and recurrence relations with respect to the degree n . Similar equations for two-matrix models are discussed in numerous papers (see, e.g., [18]).

We introduce the L -operator (the Lax operator) as multiplication by z in the basis χ_n :

$$L_{nm}\chi_m(z) = z\chi_n(z) \quad (17)$$

(summation over repeated indices is implied). Obviously, L is a lower triangular matrix with one adjacent upper diagonal, $L_{nm} = 0$ as $m > n + 1$. Similarly, the differentiation ∂_z is represented by an upper triangular matrix with one adjacent lower diagonal. Integrating by parts the matrix elements of the ∂_z , one finds:

$$(L^\dagger)_{nm}\chi_m = \hbar\partial_z\chi_n, \quad (18)$$

where L^\dagger is the Hermitian conjugate operator.

The matrix elements of L^\dagger are $(L^\dagger)_{nm} = \bar{L}_{mn} = A(L_{nm}) + \int e^{\frac{1}{\hbar}W} \bar{P}_m(\bar{z}) \partial_z P_n(z) d^2z$,

where the last term is a lower triangular matrix. The latter can be written through negative powers of the Lax operator. Writing $\partial_z \log P_n(z) = \frac{n}{z} + \sum_{k>1} v_k(n)z^{-k}$, one represents L^\dagger in the form

$$L^\dagger = A(L) + (\hbar n)L^{-1} + \sum_{k>1} v^{(k)}L^{-k}, \quad (19)$$

where $v^{(k)}$ and $(\hbar n)$ are diagonal matrices with elements $v_n^{(k)}$ and $(\hbar n)$. The coefficients $v_n^{(k)}$ are determined by the condition that lower triangular matrix elements of $A(L_{nm})$ are cancelled.

In order to emphasize the structure of the operator L , we write it in the basis of the shift operator ³ \hat{w} such that $\hat{w}f_n = f_{n+1}\hat{w}$ for any sequence f_n . Acting on the wave function, we have:

$$\hat{w}\chi_n = \chi_{n+1}.$$

In the n -representation, the operators L , L^\dagger acquire the form

$$L = r_n\hat{w} + \sum_{k\geq 0} u_n^{(k)}\hat{w}^{-k}, \quad L^\dagger = \hat{w}^{-1}r_n + \sum_{k\geq 0} \hat{w}^k \bar{u}_n^{(k)}. \quad (20)$$

Clearly, acting on χ_n , we have the commutation relation (“the string equation”)

$$[L, L^\dagger] = \hbar. \quad (21)$$

This is the compatibility condition of Eqs. (17) and (18).

Equations (20) and (21) completely determine the coefficients $v_n^{(k)}$, r_n and $u_n^{(k)}$. The first one connects the coefficients to the parameters of the potential. The second equation is used to determine how the coefficients $v_n^{(k)}$, r_n and $u_n^{(k)}$ evolve with n . In particular, the diagonal part of it reads

$$n\hbar = r_n^2 - \sum_{k\geq 1} \sum_{p=1}^k |u_{n+p}^{(k)}|^2. \quad (22)$$

Moreover, we note that all the coefficients can be expressed through the τ -function (3) and its derivatives with respect to parameters of the potential. This representation is particularly simple for r_n : $r_n^2 = \tau_n \tau_{n+1}^{-2} \tau_{n+2}$.

³ The shift operator \hat{w} has no inverse. Below \hat{w}^{-1} is understood as a shift to the left defined as $\hat{w}^{-1}\hat{w} = 1$. Same is applied to the operator L^{-1} . To avoid a possible confusion, we emphasize that although χ_n is a right-hand eigenvector of L , it is not a right-hand eigenvector of L^{-1} .

2.1 Finite dimensional reductions

If the vector potential $A(z)$ is a rational function, the coefficients $u_n^{(k)}$ are not all independent. The number of independent coefficients equals the number of independent parameters of the potential. For example, if the holomorphic part of the potential, $V(z)$, is a polynomial of degree d , the series (20) are truncated at $k = d - 1$.

In this case the semi-infinite system of linear equations (18) and the recurrence relations (17) can be cast in the form of a set of finite dimensional equations whose coefficients are rational functions of z , one system for every $n > 0$. The system of differential equations generalizes the Cristoffel-Darboux second order differential equation valid for orthogonal polynomials. This fact has been observed in recent papers [19,20] for biorthogonal polynomials emerging in the Hermitian two-matrix model with a polynomial potential. It is applicable to our case (holomorphic biorthogonal polynomials) as well.

In a more general case, when $A(z)$ is a general rational function with $d - 1$ poles (counting multiplicities), the series (20) is not truncated. However, L can be represented as a “ratio”,

$$L = K_1^{-1}K_2 = M_2M_1^{-1}, \quad (23)$$

where the operators $K_{1,2}$, $M_{1,2}$ are polynomials in \hat{w} :

$$K_1 = \hat{w}^{d-1} + \sum_{j=0}^{d-2} A_n^{(j)} \hat{w}^j, \quad K_2 = r_{n+d-1} \hat{w}^d + \sum_{j=0}^{d-1} B_n^{(j)} \hat{w}^j \quad (24)$$

$$M_1 = \hat{w}^{d-1} + \sum_{j=0}^{d-2} C_n^{(j)} \hat{w}^j, \quad M_2 = r_n \hat{w}^d + \sum_{j=0}^{d-1} D_n^{(j)} \hat{w}^j \quad (25)$$

These operators obey the relation

$$K_1M_2 = K_2M_1. \quad (26)$$

It can be proven that the pair of operators $M_{1,2}$ is uniquely determined by $K_{1,2}$ and vice versa. We note that the reduction (23) is a difference analog of the “rational” reductions of the Kadomtsev-Petviashvili integrable hierarchy considered in [21].

The linear problems (17), (18) acquire the form

$$(K_2\chi)_n = z(K_1\chi)_n, \quad (M_2^\dagger\chi)_n = \hbar\partial_z(M_1^\dagger\chi)_n. \quad (27)$$

These equations are of *finite order* (namely, of order d), i.e., they connect values of χ_n on $d + 1$ subsequent sites of the lattice.

The semi-infinite set $\{\chi_0, \chi_1, \dots\}$ is then a “bundle” of d -dimensional vectors

$$\underline{\chi}(n) = (\chi_n, \chi_{n+1}, \dots, \chi_{n+d-1})^t$$

(the index t means transposition, so $\underline{\chi}$ is a column vector). The dimension of the vector is the number of poles of $A(z)$ plus one. Each vector obeys a closed d -dimensional linear differential equation

$$\hbar \partial_z \underline{\chi}(n) = \mathcal{L}_n(z) \underline{\chi}(n), \quad (28)$$

where the $d \times d$ matrix \mathcal{L}_n is a “projection” of the operator L^\dagger onto the n -th d -dimensional space. Matrix elements of the \mathcal{L}_n are rational functions of z having the same poles as $A(z)$ and also a pole at the point $\overline{A(\infty)}$. (If $A(z)$ is a polynomial, all these poles accumulate to a multiple pole at infinity).

We briefly describe the procedure of constructing the finite dimensional matrix differential equation. We use the first linear problem in (27) to represent the shift operator as a $d \times d$ matrix $\mathcal{W}_n(z)$ with z -dependent coefficients:

$$\mathcal{W}_n(z) \underline{\chi}(n) = \underline{\chi}(n+1). \quad (29)$$

This is nothing else than rewriting the scalar linear problem in the matrix form. Then the matrix $\mathcal{W}_n(z)$ is to be substituted into the second equation of (27) to determine $\mathcal{L}_n(z)$ (examples follow). The entries of $\mathcal{W}_n(z)$ and $\mathcal{L}_n(z)$ obey the Schlesinger equation, which follows from compatibility of (28) and (29):

$$\hbar \partial_z \mathcal{W}_n = \mathcal{L}_{n+1} \mathcal{W}_n - \mathcal{W}_n \mathcal{L}_n. \quad (30)$$

This procedure has been realized explicitly for polynomial potentials in recent papers [19,20]. We will work it out in detail for our three examples: $\underline{\chi}(n) = (\chi_n, \chi_{n+1})^t$ for the ellipse (6) and the aircraft wing (7) and $\underline{\chi}(n) = (\chi_n, \chi_{n+1}, \chi_{n+2})^t$ for the hypotrochoid (8).

2.2 Spectral curve

According to the general theory of linear differential equations, the semiclassical (WKB) asymptotics of solutions to Eq. (28), as $\hbar \rightarrow 0$, is found by solving the eigenvalue problem for the matrix $\mathcal{L}_n(z)$ (see, e.g., [22]). More precisely, the basic object of the WKB approach is the spectral curve [23] of the matrix \mathcal{L}_n , which is defined, for every integer $n > 0$, by the secular equation $\det(\mathcal{L}_n(z) - \tilde{z}) = 0$ (here \tilde{z} means $\tilde{z} \cdot \mathbf{1}$, where $\mathbf{1}$ is the unit $d \times d$ matrix). It is clear that the left hand side of the secular equation is a polynomial in \tilde{z} of degree d . We define the spectral curve by an equivalent equation

$$f_n(z, \tilde{z}) = a(z) \det(\mathcal{L}_n(z) - \tilde{z}) = 0, \quad (31)$$

where the factor $a(z)$ is added to make $f_n(z, \tilde{z})$ a polynomial in z as well. The factor $a(z)$ then has zeros at the points where poles of the matrix function $\mathcal{L}(z)$ are located. It does not depend on n . We will soon see that the degree of the polynomial $a(z)$ is equal to d . Assume that all poles of $A(z)$ are simple, then zeros of the $a(z)$ are just the $d - 1$ poles of $A(z)$ and another simple zero at the point $\overline{A(\infty)}$. Therefore, we conclude that the matrix $\mathcal{L}_n(z)$ is rather special. For a general $d \times d$ matrix function with the same d poles, the factor $a(z)$ would be of degree d^2 .

Note that the matrix $\mathcal{L}_n(z) - \bar{z}$ enters the differential equation

$$\hbar \partial_z |\underline{\psi}(n)|^2 = \overline{\underline{\psi}}(n) (\mathcal{L}_n(z) - \bar{z}) \underline{\psi}(n) \quad (32)$$

for the squared amplitude $|\underline{\psi}(n)|^2 = \underline{\psi}^\dagger(n) \underline{\psi}(n) = e^{-\frac{|z|^2}{\hbar}} |\underline{\chi}(n)|^2$ of the vectors $\underline{\psi}(n)$ built from the orthonormal wave functions (14).

The equation of the curve can be interpreted as a “resultant” of the non-commutative polynomials $K_2 - zK_1$ and $M_2^\dagger - \tilde{z}M_1^\dagger$ (cf. [19]). Indeed, the point (z, \tilde{z}) belongs to the curve if and only if the linear system

$$\left\{ \begin{array}{l} (K_2 c)_k = z(K_1 c)_k \quad n - d \leq k \leq n - 1 \\ (M_2^\dagger c)_k = \tilde{z}(M_1^\dagger c)_k \quad n \leq k \leq n + d - 1 \end{array} \right. \quad (33)$$

has non-trivial solutions. The system contains $2d$ equations for $2d$ variables $c_{n-d}, \dots, c_{n+d-1}$. Vanishing of the $2d \times 2d$ determinant yields the equation of the spectral curve. Below we use this method to find the equation of the curve in the examples. It appears to be much easier than the determination of the matrix $\mathcal{L}_n(z)$.

The spectral curve (31) possesses an important property: it admits an antiholomorphic involution. In the coordinates z, \tilde{z} the involution reads $(z, \tilde{z}) \mapsto (\overline{\tilde{z}}, \overline{z})$. This simply means that the secular equation $\det(\overline{\mathcal{L}}_n(\tilde{z}) - z) = 0$ for the matrix $\overline{\mathcal{L}}_n(\tilde{z}) \equiv \overline{\mathcal{L}_n(\tilde{z})}$ defines the same curve. Therefore, the polynomial f_n takes real values for $\tilde{z} = \overline{z}$:

$$f_n(z, \overline{z}) = \overline{f_n(\overline{z}, z)}. \quad (34)$$

Points of the real section of the curve ($\tilde{z} = \overline{z}$) are fixed points of the involution.

The curve (31) was discussed in recent papers [19,20] in the context of Hermitian two-matrix models with polynomial potentials. The dual realizations of the curve pointed out in [19] correspond to the antiholomorphic involution in our case. The involution can be proven along the lines of these works. The proof is rather technical and we omit it, restricting ourselves to the examples

below. We simply note that the involution relies on the fact that the squared modulus of the wave function is real.

2.3 Schwarz function

The polynomial $f_n(z, \bar{z})$ can be factorized in two ways:

$$f_n(z, \bar{z}) = a(z)(\bar{z} - S_n^{(1)}(z)) \dots (\bar{z} - S_n^{(d)}(z)), \quad (35)$$

where $S_n^{(i)}(z)$ are eigenvalues of the matrix $\mathcal{L}_n(z)$, or

$$f_n(z, \bar{z}) = \overline{a(z)}(z - \bar{S}_n^{(1)}(\bar{z})) \dots (z - \bar{S}_n^{(d)}(\bar{z})), \quad (36)$$

where $\bar{S}_n^{(i)}(\bar{z})$ are eigenvalues of the matrix $\bar{\mathcal{L}}_n(\bar{z})$. One may understand them as different branches of a multivalued function $S(z)$ (respectively, $\bar{S}(z)$) on the plane (here we do not indicate the dependence on n , for simplicity of the notation). It then follows that $S(z)$ and $\bar{S}(z)$ are mutually inverse functions:

$$\bar{S}(S(z)) = z. \quad (37)$$

An algebraic function with this property is called *the Schwarz function*. By the equation $f(z, S(z)) = 0$, it defines a complex curve with an antiholomorphic involution. An upper bound for genus of this curve is $g = (d - 1)^2$, where d is the number of branches of the Schwarz function. The real section of this curve is a set of all fixed points of the involution. It consists of a number of contours on the plane (and possibly a number of isolated points, if the curve is not smooth). The structure of this set is known to be complicated. Depending on coefficients of the polynomial, the number of disconnected contours in the real section may vary from 0 to $g + 1$. If the contours divide the complex curve into two disconnected “halves”, or sides (related by the involution), then the curve can be realized as the *Schottky double* [24,25,26] of one of these sides. Each side is a Riemann surface with a boundary.

We will discuss general properties of the Schwarz function and the Schottky double in Sec. 4.

Let us come back to equation (28). It has d independent solutions. They are functions on the spectral curve. One of them is a physical solution corresponding to biorthogonal polynomials. The physical solution defines the “physical sheet” of the curve.

The Schwarz function on the physical sheet is a particular root, say $S_n^{(1)}(z)$, of the polynomial $f_n(z, \bar{z})$ (see (35)). It follows from (19) that this root is selected by the requirement that it has the same poles and residues as the potential A .

A formal ⁴ semiclassical asymptote of the solution, in the leading order in \hbar , is

$$\chi_n \sim e^{\frac{1}{\hbar} \int^z d\Omega_n^{(1)}}. \quad (38)$$

Here

$$d\Omega_n^{(1)} = S_n^{(1)} dz.$$

The differential $d\Omega_n^{(1)}$ is a physical branch of the generating differential on the curve (see below).

The semiclassical asymptotics is discussed in more details in Sec. 6. Here we notice that the amplitude of the wave function $\psi_n(z)$ (not $\chi_n(z)$!) peaks at the solution of the equation

$$S^{(1)}(z) = \bar{z}, \quad (39)$$

where now $z = x + iy$ and $\bar{z} = x - iy$ are complex conjugated coordinates in the plane. Solutions to this equation describe those contours of a real section of the complex curve which belong to the physical sheet. It is a set of closed planar curves, as shown in Fig. 1. These curves are boundaries of semiclassical droplets. Evolution and growth of the droplets translate into evolution of the complex curve.

2.4 Deformation parameters

The essential information about the spectral curve (which, in what follows, we will call *quantum curve*, unless the semiclassical limit is considered) is contained in two conditions:

- the antiholomorphic involution, and
- poles and residues of the Schwarz function on one selected sheet (the physical sheet) are given by the vector potential field $A(z)$.

These requirements determine all but g coefficients of the polynomial $f_n(z, \bar{z})$, where g is genus of the curve. The remaining g coefficients do not depend on the potential (deformation parameters).

The Bohr-Sommerfeld quantization condition for the semiclassical wave function (38) requires that the integral over all the cuts (or boundaries of the droplets) are integer multiples of $2\pi i$. Also, the integral around the point at infinity, counting the degree of the polynomial, must be $2\pi i N$. The integrals over the cuts transform into the integrals over **a**-cycles of the curve. Later we

⁴ This formal expression ignores the Stokes phenomenon. It is valid only around boundaries of physical droplets.

will interpret the \mathbf{a} -cycles as boundaries of the droplets. Therefore, we have the set of integers

$$\nu_a = \frac{1}{2\pi i \hbar} \oint_{\mathbf{a}_\alpha} S(z) dz, \quad \sum_\alpha \nu_\alpha = N, \quad \alpha = 0, 1, \dots, g. \quad (40)$$

The d -dimensional linear differential equations (28) give an interpretation of the potential data as deformation parameters. Varying the poles and residues of $A(z)$, one does not change the monodromy of solutions, given by N and ν_α . They are similar to deformation parameters of the theory of isomonodromic deformations of the system of linear differential equations [27] (see also Ref. [8] for applications of the theory of isomonodromic deformations to Hermitian matrix models and orthogonal polynomials in one variable, and references therein). A connection between isomonodromic deformations and Whitham equations, which seems to be relevant to our discussion, was pointed out in Ref. [28].

In the spirit of the theory of isomonodromic deformations of linear differential equations, we conjecture that a specific value of N , a potential $V(z)$, and a set of g numbers (40) form a complete data set which uniquely determines the coefficients $r_n, u_n^{(k)}$ of the recurrence equations, and the solution of the differential equation (28). We do not know, however, whether the requirement that the physical solutions are polynomials gives a restriction on possible values of the integers ν_α . It is likely that a general set of ν_α (positive and negative) corresponds to more general solutions of (28) rather than polynomials.

We also conjecture that, for physical values of the parameters of the potential in general position, the quantum curve is smooth (i.e., non-degenerate), and has the maximal possible number of the disconnected closed contours (“real ovals”) in the real section. In the latter case, the involution is known to divide the complex curve into two “halves”, thus making the Schottky double construction applicable.

Before discussing general properties of the curve, we illustrate its appearance in the semiclassical limit.

3 Semiclassical curve

By semiclassical case we mean the limit $N \rightarrow \infty, \hbar \rightarrow 0$, while the time $t = \hbar N$, and the potential remain fixed. In this case, all eigenvalues are distributed continuously within droplets with sharp boundaries. The boundary of the droplets is a real section of the *classical curve*.

3.1 Saddle point equation and Riemann-Hilbert problem

In the semiclassical limit, the distribution (2) peaks at the minimum of the function $W(z) - \varphi(z)$, where

$$\varphi(z) = -\hbar \sum_{i=1}^N \log |z - z_i|^2$$

is the Newton potential, logarithmic in 2-D, of the domain (the support of eigenvalues). In the semiclassical limit, the potential φ is continuous. One writes the extremum condition in the form

$$\partial_z (\varphi - W) = \partial_{\bar{z}} (\varphi - W) = 0, \quad \text{at } z = z_i. \quad (41)$$

The points where this equations holds are the most probable positions of eigenvalues z_i .

In addition, if one assumes that z_i have a continuous distribution (a strong assumption), i.e., that the density

$$\rho_N(z) = \hbar \sum_{i=1}^N \delta(z - z_i) = -\frac{1}{4\pi} \Delta \varphi \quad (42)$$

is a smooth positive function in some domain D , and zero outside this domain, then it follows from (41) that the density is $-\frac{1}{4\pi} \Delta W$ inside the domain, if $-\Delta W$ is not singular and positive inside the support of eigenvalues.

The shape of the domain is found in two steps. First, one finds the potential φ . Then, having the potential, one has to restore the shape of the domain. The second step is the *inverse potential problem*.

Under this assumption, φ is a harmonic function in the exterior of the support of eigenvalues. Then equation (41) reads as a Riemann-Hilbert problem:

- (i) The boundary value of the analytic function $\partial_z \varphi$ in the exterior of the domain D is $\partial_z W$;
- (ii) The function $\partial \varphi$ behaves at infinity as $-\hbar N z^{-1} = -t/z$ (we assume that there are no eigenvalues around infinity).

These conditions uniquely specify the domain if it is simply connected. In this case, $\pi \hbar N$ is the area of the domain. Multiply-connected domains are also possible solutions. The number of disconnected droplets cannot exceed the number of poles of $A(z)$ plus one. To find them one needs additional data. For example, one may fix the filling factors – the number of eigenvalues that each droplet contains. Obviously, all the filling factors are positive and their

sum is N . Domains constructed this way, provided $A(z)$ is a rational function, belong to a special class of *algebraic domains* [29].

An important property of the Riemann-Hilbert problem is that the function $\partial\varphi(z)$, with z inside the domain, does not depend on N , but rather on the potential. The former does not change during the growth.

At this point, we specify the potential to be of the form (4). Then the boundary value of the analytic function $\partial\varphi(z)$ is $\partial W = -\bar{z} + A(z)$. The density of eigenvalues is uniform, and the filling factors fix the areas of the droplets to be $\pi\hbar\nu_\alpha$.

The potential $\varphi(z)$ can be constructed with the help of the Schwarz function.

3.2 The Schwarz function and the inverse potential problem

Given a closed (in general a multiply-connected) domain D in the plane, the *Schwarz function* $S(z)$ is an analytic function in some neighborhood of the boundary of the domain with the value \bar{z} on the boundary [24]:

$$S(z) = \bar{z} \quad \text{on the contour.} \quad (43)$$

The involution property of the Schwarz function follows from the definition (cf. (37)):

$$\bar{S}(S(z)) = z.$$

Let us represent the Schwarz function in the form $S(z) = S_+(z) + S_-(z)$, where S_+ (respectively, S_-) is analytic inside (respectively, outside) D , with the condition that $S_-(\infty) = 0$. Choose $S_+(z)$ to be equal to $A(z)$,

$$A(z) = \frac{1}{2\pi i} \oint_{\partial D} \frac{\bar{\zeta} d\zeta}{z - \zeta}, \quad z \in D. \quad (44)$$

Then the function $S_-(z) = S(z) - A(z)$, being analytic outside D , has the boundary value $\bar{z} - A(z)$. We conclude that $A(z) - S(z) = \partial\varphi(z)$.

Therefore, the problem of the previous section reads: given a potential $A(z)$, find the Schwarz function

$$S(z) = A(z) + S_-(z) \quad (45)$$

whose poles and residues outside of the support of eigenvalues are given by the poles and residues of $A(z)$ and such that $S_-(z) \rightarrow \hbar N/z$ as $z \rightarrow \infty$. If the Schwarz function is known, Eq. (43) determines the domain. Inside the droplet $S_-(z)$, and therefore, $S(z)$ have cuts (Fig. 8).

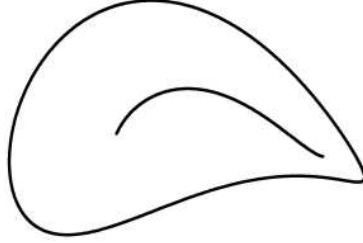


Fig. 8. The boundary of a droplet and a cut of the Schwarz function located inside the droplet.

A note is in order. In Sec. 3.1 we assumed that the density of eigenvalues is a continuous function everywhere except for the boundary of D . As a consequence, φ is a harmonic function, $\partial\varphi$ and $S_-(z)$ are analytic functions outside D , and the Schwarz function outside the droplets has the same poles as $A(z)$. As a result, the complement to the support of eigenvalues appears to be an algebraic domain.

It seems that this assumption is too restrictive. Moreover, the definition of the curve through the linear differential equations for the wave function of Sec. 2.2 does not forbid the physical branch of the Schwarz function to have branching points and cuts outside physical droplets, as shown in Figs. 3, 4. The semiclassical wave function still peaks on the real section of the curve (39), regardless of whether there are cuts outside the droplets, or if those cuts shrink to points. In other words, a solution with cuts outside physical droplets still has a local maximum on the boundary of the physical droplets and it is stable. It becomes unstable, however, in a vicinity of cuts along a normal direction to a cut.

These arguments suggest that one can safely allow $\partial\varphi(z)$ to have branching points, i.e., the Schwarz function is allowed to have cuts outside physical droplets. Then we seek for solutions of the Riemann-Hilbert problem of Sec. 3.1 in a wider class of functions. This leads to a wider class of domains (not algebraic). However, in this case, one is no longer able to treat eigenvalues as continuously distributed. We will come back to this issue in the next section.

4 The Schwarz function and its Riemann surface. The Schottky double.

The Schwarz function describes more than just the boundary of clusters of eigenvalues. Together with other sheets it defines a Riemann surface. If the potential $A(z)$ is meromorphic, the Schwarz function is an algebraic function. It satisfies a polynomial equation $f(z, S(z)) = 0$.

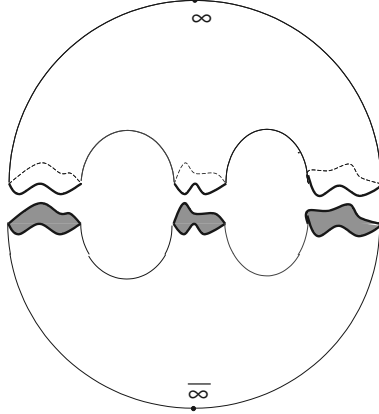


Fig. 9. The Schottky double. A Riemann surface with boundaries along the droplets (a front side) is glued to its mirror image (a back side).

The function $f(z, \tilde{z})$, where z and \tilde{z} are treated as two independent complex arguments, defines a Riemann surface with antiholomorphic involution (34). If the involution divides the surface into two disconnected parts, as explained above, the Riemann surface is the *Schottky double* [25,26] of one of these parts.

There are two complementary ways to describe this surface. One is through the algebraic covering (35, 36). Among d sheets we distinguish a *physical* sheet. The physical sheet is selected by the condition that the differential $S(z)dz$ has the same poles and residues as the differential of the potential $A(z)dz$ (as in (45)). It may happen that the condition $\bar{z} = S^{(i)}(z)$ defines a planar curve (or several curves, or a set of isolated points) for branches other than the physical one. We refer to the interior of these planar curves as *virtual* (or unphysical) droplets situated on sheets other than physical.

Another way emphasizes the antiholomorphic involution. Consider a meromorphic function $h(z)$ defined on a Riemann surface with boundaries. We call this surface the front side. The Schwarz reflection principle extends any meromorphic function on the front side to a meromorphic function on the Riemann surface without boundaries. This is done by adding another copy of the Riemann surface with boundaries (a back side), glued to the front side along the boundaries, Fig 9. The value of the function h on the mirror point on the back side is $h(\overline{S(z)})$. The copies are glued along the boundaries: $h(z) = h(\overline{S(z)})$ if the point z belongs to the boundary. The same extension rule applies to differentials. Having a meromorphic differential $h(z)dz$ on the front side, one extends it to a meromorphic differential $h(\overline{S(z)})d\overline{S(z)}$ on the back side.

This definition can be applied to the Schwarz function itself. We say that the Schwarz function on the double is $S(z)$ if the point is on the front side, and \bar{z} if the point belongs to the back side (here we understand $S(z)$ as a function defined on the complex curve, not just on the physical sheet).

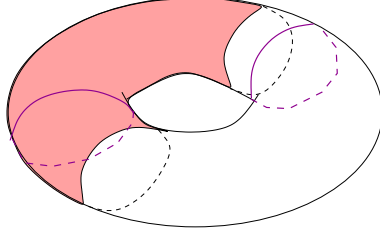


Fig. 10. Physical and unphysical droplets on a torus. The physical sheet (shaded) meets the unphysical sheet along the cuts. The cut situated inside the unphysical droplet appears on the physical sheet. The boundaries of the droplets (physical and virtual) belong to different sheets. This torus is the Riemann surface corresponding to the ensemble with the potential $V(z) = -\alpha \log(1 - z/\beta) - \gamma z$.

The number of sheets of the curve is the number of poles (counted with their multiplicity) of the function $A(z)$ plus one. Indeed, according to (45) poles of A are poles of the Schwarz function on the front side of the double. On the back side, there is also a pole at infinity. Since $S(z = \infty) = A(\infty)$, we have $\bar{S}(\bar{z} = A(\infty)) = \infty$. Therefore, the factor $a(z)$ is a polynomial with zeros at the poles of $A(z)$ and at $\overline{A(\infty)}$, and

$$d \equiv \text{number of sheets} = \text{number of poles of } A + 1.$$

The front and back sides meet at planar curves $\bar{z} = S(z)$. These curves are boundaries of the droplets. We repeat that not all droplets are physical. Some of them may belong to unphysical sheets, Fig. 10.

Boundaries of droplets, physical and virtual, form a subset of the **a**-cycles on the curve. Their number cannot exceed the genus of the curve plus one:

$$\text{number of droplets} \leq g + 1.$$

The sheets meet along cuts located inside droplets. The cuts that belong to physical droplets show up on unphysical sheets. On the other hand, some cuts show up on the physical sheet (Fig 10). They correspond to droplets situated on unphysical sheets.

The Riemann-Hurwitz theorem computes the genus of the curve as

$$g = \text{half the number of branching points} - d + 1.$$

With the help of the Stokes formula, the numbers $\{\nu_\alpha\}$ are identified with areas of the droplets: $|\nu_\alpha| = \frac{1}{2\pi\hbar} \int_{D_\alpha} d^2z$. For a nondegenerate curve, these numbers are not necessarily positive. Negative numbers correspond to droplets located on unphysical sheets. In this case, $\{\nu_\alpha\}$ do not correspond to the number of eigenvalues located inside each droplet, as it is the case for algebraic domains, when all filling numbers are positive.

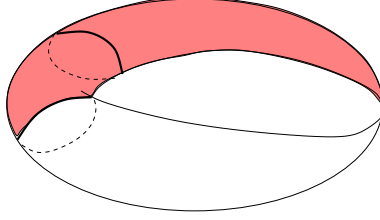


Fig. 11. Degenerate torus corresponds to the algebraic domain for the Joukowski map.

A comment is in order. In the Hermitian or unitary one-matrix ensembles, the construction of the Riemann surface is different (Refs. [4,10,11,30]). In the Hermitian random matrix ensemble, for example, eigenvalues are real. The support of eigenvalues is a set of disjoint intervals on the real line. In this case, branch cuts are identical to the support of eigenvalues. The Riemann surface is constructed by gluing g sheets along $g + 1$ cuts [30]. Conversely, in the Schottky double the cuts generally do not touch boundaries of the droplets (Fig. 8). Complex curves for the Hermitian or unitary ensembles are simpler. They are always hyperelliptic.

4.1 Degeneration of the spectral curve

Degeneration of the complex curve gives the most interesting physical aspects of growth. There are several levels of degeneration. We briefly discuss them below.

4.1.1 Algebraic domains and double points

A special case occurs when the Schwarz function on the physical sheet is meromorphic. It has no other singularities than poles of A . This is the case of algebraic domains [29]. They appear in the semiclassical case (see Sec. 3). This situation occurs if cuts on the physical sheet, situated outside physical droplets, shrink to points, i.e., two or more branching points merge. Then the physical sheet meets other sheets along cuts situated inside physical droplets only and also at some points on their exterior (*double points*) (see figure captions for Figs. 3, 4). In this case the Riemann surface degenerates. The genus is given by the number of physical droplets only. The filling factors (40) are all positive.

In the case of algebraic domains, the physical branch of the Schwarz function is a well-defined meromorphic function. Analytic continuations of \bar{z} from different disconnected parts of the boundary give the same result. In this case, the Schwarz function can be written through the Cauchy transform of the

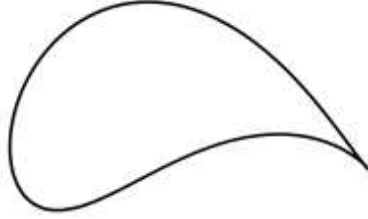


Fig. 12. Critically degenerate Joukowski map.

physical droplets:

$$S(z) = A(z) + \frac{1}{\pi} \int_D \frac{d^2\zeta}{z - \zeta}. \quad (46)$$

Although algebraic domains occur in physical problems such as Laplacian growth, their semiclassical evolution is limited. Almost all algebraic domains will be broken in a growth process. Within a finite time (the area of the domain) they degenerate further into critical curves (Fig. 7, 12). The Gaussian potential (the Ginibre-Girko ensemble), which leads to a single droplet of the form of an ellipse is a known exception.

4.1.2 Critical degenerate curves

Algebraic domains appear as a result of merging of simple branching points on the physical sheet. The double points are located outside physical droplets. Remaining branching points belong to the interior of physical droplets. Initially, they survive in the degeneration process. However, as known in the theory of Laplacian growth, the process necessarily leads to a further degeneration. Sooner or later, at least one of the interior branching points merges with one of the double points in the exterior. Curves degenerated in this manner are called *critical*. For the genus one and three this degeneration is discussed below. The critical degenerations are depicted, respectively, in Fig. 12 and Fig. 7.

Since interior branching points can only merge with exterior branching points on the boundary of the droplet, the boundary develops a cusp, characterized by a pair p, q of mutually prime integers. In local coordinates around such a cusp, the curve looks like $x^p \sim y^q$.

The fact that the growth of algebraic domains always leads to critical curves is known in the theory of Laplacian growth (see e.g., [31]) as finite time singularities. It is also known in the Hermitian one- and two-matrix models as critical points (intensively studied in 2-D-gravity [7]).

The degeneration process seems to be a feature of the semiclassical approximation. Curves treated beyond this approximation never degenerate.

4.1.3 Simply-connected domains. Conformal maps.

The case when the complement to the support of eigenvalues is a simply-connected algebraic domain in the extended (i.e. including ∞) complex plane is particularly important. All the filling factors are zero except one, which is equal to N , so there is only one droplet D . In this case, the Schottky double of the exterior of the droplet is a Riemann sphere.

The exterior domain can be conformally and univalently mapped onto the exterior of the unit disc. We call this map $w(z)$, and its inverse $z(w)$. For algebraic domains, the inverse map is a rational function of w . Choosing the normalization such that $z(\infty) = \infty$, we represent the inverse map by a half-infinite Laurent polynomial

$$z(w) = rw + \sum_{k>0} u_k w^{-k}, \quad |w| \geq 1. \quad (47)$$

The coefficient r , called the external conformal radius of the domain D , is chosen to be real positive. The Schwarz reflection of the inverse map is

$$\bar{z}(w^{-1}) = rw^{-1} + \sum_{k>0} \bar{u}^{(k)} w^k, \quad |w| \geq 1. \quad (48)$$

Given a point z , there are d values of w solving the equation (47), where d is the number of poles of the rational function $z(w)$. Among them, only one solution corresponds to the conformal map. It is the solution such that $w \rightarrow z/r$ as $z \rightarrow \infty$. The global coordinate w on the Riemann sphere provides a uniformization of the Schottky double. In this coordinate, the involution reads $w \rightarrow 1/\bar{w}$. The Schwarz function is

$$S(z) = \bar{z}(w^{-1}(z)). \quad (49)$$

Choose a regular point ξ_0 of the potential inside the droplet and expand

$$V(z) = \sum_{k>0} t_k (z - \xi_0)^k. \quad (50)$$

The coefficients t_k have a simple geometric interpretation. It follows from (44) that they are *harmonic moments* of the exterior of the droplet (with respect to the point ξ_0):

$$t_k = -\frac{1}{\pi k} \int_{C \setminus D} (z - \xi_0)^{-k} d^2 z. \quad (51)$$

We also mention the area formula

$$t = r^2 - \sum_{k \geq 1} k |u^{(k)}|^2. \quad (52)$$

If the vector potential $A(z)$ is a polynomial of degree $d - 1$, then the inverse map $z(w)$ is a (Laurent) polynomial: $u^{(k)} = 0$, $k > d - 1$. If $A(z)$ is a rational function with $d - 1$ simple poles in the finite part of the complex plane, the map $z(w)$ is a rational function with $d - 1$ simple poles and one extra simple pole at infinity.

4.2 The generating differential

The meromorphic differential

$$d\Omega = S(z)dz \quad (53)$$

plays an important role. It is called generating differential [3,32]. According to (45), on the physical sheet it has the same poles and residues as the differential Adz :

$$d\Omega = Adz + S_-(z)dz. \quad (54)$$

Below we use the following properties of the generating differential.

- (i) The periods over \mathbf{a} -cycles (boundaries of the droplets) are purely imaginary, and are integer multiples of $2\pi i$. They compute areas of the droplets (the filling factors (40)):

$$\nu_\alpha = \frac{1}{2\pi i\hbar} \oint_{\mathbf{a}_\alpha} d\Omega.$$

The filling factors of physical droplets (belonging to the physical sheet) are positive.

- (ii) The real part of the integral of the differential $(\bar{z} - S(z))dz$ from some fixed point ξ_0 to a point on the boundary of a droplet (a point on a \mathbf{a} -cycle) has the same value for all points of the boundary:

$$\phi_\alpha = -|z|^2 + 2\mathcal{R}e \int_{\xi_0}^z d\Omega = \text{const}, \quad \text{for all } z \in \mathbf{a}_\alpha.$$

This quantity does not depend on z , but does depend on ξ_0 unless ξ_0 is on the boundary. However, the difference $\phi_\alpha - \phi_\beta$ depends on the \mathbf{a} -cycles only. It is equal to a \mathbf{b} -period of the differential $d\Omega$:

$$\phi_\alpha - \phi_\beta = \oint_{\mathbf{b}_{\alpha\beta}} d\Omega, \quad (55)$$

where $\mathbf{b}_{\alpha\beta}$ is a cycle connecting \mathbf{a}_α and \mathbf{a}_β cycles.

For proofs and more details, see Ref. [3].

Periods over \mathbf{b} -cycles $\phi_\alpha - \phi_0$ play a role of chemical potentials for the filling factors. Here 0 denotes a chosen reference droplet. One can use chemical

potentials to characterize evolution of the curve instead of filling factors.

5 Examples

5.1 Genus zero – ellipse

The potential is Gaussian, $V(z) = t_2 z^2$, $2|t_2| < 1$, $A(z) = 2t_2 z$. It has a simple pole at infinity. The number of sheets of the Schwarz function is two. At infinity, $S'(z)$ is finite. Therefore, $S'(z)$ takes every value twice. It must have two zeros at most, i.e., there are two branching points. The Riemann-Hurwitz theorem says that genus is zero. The curve with two branching points and two sheets has the form $f(z, \bar{z}) = z\bar{z} + k_1 z^2 + \bar{k}_1 \bar{z}^2 + k_2 = 0$. Conditions that $S(z) \sim 2t_2 z + n\hbar z^{-1} + \dots$ at $z \rightarrow \infty$ for the physical branch and the unitarity condition (37) determine the curve in full:

$$f_n(z, \bar{z}) = z\bar{z} - (t_2 z^2 + \bar{t}_2 \bar{z}^2) \frac{2}{1 + 4|t_2|^2} - n\hbar \frac{1 - 4|t_2|^2}{1 + 4|t_2|^2} = 0. \quad (56)$$

The physical branch

$$S^{(1)}(z) = 2t_2 z + \frac{(2\bar{t}_2)^{-1} - 2t_2}{2} z \left(1 - \sqrt{1 - \frac{2}{(2\bar{t}_2)^{-1} - 2t_2} \frac{2n\hbar}{z^2}} \right)$$

is the Schwarz function of ellipse. The second branch $S^{(2)}(z) \rightarrow (2\bar{t}_2)^{-1} z$ does not correspond to any real curve. The droplet (see Fig. 2) is an ellipse with the quadrupole moment $2|t_2|$ and area $\pi t = \pi n\hbar$.

Recurrence relations Eqs. (20, 18) truncate

$$z\psi_n = r_n \psi_{n+1} + u_n \psi_{n-1}, \quad (L^\dagger \psi)_n = r_{n-1} \psi_{n-1} + \bar{u}_{n+1} \psi_{n+1}. \quad (57)$$

Equations (19, 22) imply

$$2t_2 = \frac{\bar{u}_{n+1}}{r_n}, \quad n\hbar = r_n^2 - |u_{n+1}|^2, \quad (58)$$

where the second equation is an analog of the area formula (52). Together they give a growth equation for the quantum analog of conformal radius $n\hbar = (1 - |2t_2|^2)r_n^2$.

The operator L^\dagger can be cast in the form of a 2×2 matrix (the number of sheets of the curve). Writing (57) for $n+1$, we express χ_{n-1} and χ_{n+2} through $\underline{\chi}_n = (\chi_n, \chi_{n+1})$ from the first pair, and substituting them to the second pair

we obtain

$$\mathcal{L}_n \underline{\chi}_n = \begin{pmatrix} z \frac{r_{n-1}}{u_n} & \bar{u}_{n+1} - \frac{r_n r_{n-1}}{u_n} \\ r_n - \frac{\bar{u}_{n+2} u_{n+1}}{r_{n+1}} & \frac{\bar{u}_{n+2}}{r_{n+1}} z \end{pmatrix} \underline{\chi}_n. \quad (59)$$

Formally, one can say that the recurrence relation (57) represents the shift operator as the 2×2 matrix

$$\mathcal{W}_{n-1} = \begin{pmatrix} 0 & 1 \\ -\frac{u_n}{r_n} & \frac{z}{r_n} \end{pmatrix}.$$

The relation $\mathcal{L}_n = \begin{pmatrix} r_{n-1} & 0 \\ 0 & r_n \end{pmatrix} \mathcal{W}_{n-1}^{-1} + \begin{pmatrix} \bar{u}_{n+1} & 0 \\ 0 & \bar{u}_{n+2} \end{pmatrix} \mathcal{W}_n$ then yields (59).

With the help of (58), \mathcal{L}_n reads

$$\mathcal{L}_n(z) = \begin{pmatrix} z(2\bar{t}_2)^{-1} & -r_n(2\bar{t}_2)^{-1}(1 - 4|t_2|^2) \\ r_n(1 - 4|t_2|^2) & 2t_2 z \end{pmatrix}.$$

Computing the determinant $\det(\mathcal{L}_n(z) - \bar{z})$, we obtain the curve (56), already determined by the singularities.

The recurrence relation can be used to generate the Hermite polynomials. The model with potential $V(z) = t_2 z^2 + Q \log z$ can also be solved explicitly (Ref. [39]). It generates the Laguerre polynomials. These are the cases where biorthogonal polynomials are classical orthogonal polynomials.

Classical polynomials correspond to a genus zero curve. Higher genus curves generate more complicated, but more interesting polynomials.

The classical limit of the recurrence relations gives a conformal map of the exterior of the unit disk to the exterior of the ellipse, $z(w) = rw + \frac{u}{w}$. The double-valued function $w_{1,2}(z) = \frac{1}{2r} \left[z \pm \sqrt{(z - z_1)(z - z_2)} \right]$, $z_{1,2} = \pm 2\sqrt{ur}$ becomes single-valued on a two-sheet covering of the z -sphere plane. The branch $w_1(z)$ is such that $w_1 \rightarrow \infty$ as $z \rightarrow \infty$. It defines the inverse map from the ellipse exterior onto the exterior of the unit disk in the w -plane. The function $\bar{z}(w^{-1}) = rw^{-1} + \bar{u}w$ is a meromorphic function of w with one simple pole at $w = 0$. Treated as functions of z , the two sheets $S^{(1,2)}(z) = \bar{z}(w_{1,2}^{-1}(z))$ have two critical points $z_{1,2}$ and constitute a sphere. Parameters of the map are related to the parameters of the potential through the classical limit of (58): $t_2 = \frac{\bar{u}}{2r}$, $t = r^2 - |u|^2$. The general formula for the semiclassical behavior of the wave function (76) gives the known asymptotics of the Hermite polynomials [34].

The cut inside the droplet may shrink to a point. In this case only one (physi-

cal) sheet remains, and the Schwarz function becomes a rational function with one simple pole. The wave functions are monomials. The droplet is a disk.

A more interesting degeneration occurs at the critical value of $|t_2| = \frac{1}{2}$, when the two branching points reach the boundary of the droplet. The ellipse degenerates into the cut $[z_1, z_2]$.

Beyond the critical value ($|t_2| > \frac{1}{2}$), the ellipse appears again, but on the unphysical sheet. In this case, there is no physical droplet, but there is a virtual droplet. At this value of t_2 , the matrix integral diverges, but a solution of the differential equation (28) exists. It is not a polynomial, however.

Below we use a more direct method to find the quantum curve bypassing the matrix representation of L^\dagger . The method reflects the triangular structure of L^\dagger , and closely resembles the procedure used in the classical case. We will use this method for the following, more complicated, examples.

Apply (57) to an eigenvector c_n of the matrix $\mathcal{L}_n(z)$ with an eigenvalue \tilde{z} . The equations

$$\begin{cases} z c_n = r_n c_{n+1} + u_n c_{n-1} \\ \tilde{z} c_n = \bar{u}_{n+1} c_{n+1} + r_{n-1} c_{n-1} \end{cases}$$

are compatible if the point (z, \tilde{z}) belongs to the curve. To obtain a compatibility condition, we express c_{n+1} and c_{n-1} in terms of c_n . The results must differ by a shift $n \rightarrow n + 2$

$$\det \begin{vmatrix} z & u_n \\ \bar{z} & r_{n-1} \end{vmatrix} \det \begin{vmatrix} r_{n+1} & z \\ \bar{u}_{n+2} & \bar{z} \end{vmatrix} = d_n d_{n+1}, \quad d_n = \det \begin{vmatrix} r_n & u_n \\ \bar{u}_{n+1} & r_{n-1} \end{vmatrix}.$$

This gives the curve (56).

5.2 Genus one – an aircraft wing

The potential is $V(z) = -\alpha \log(1 - z/\beta) - \gamma z$, $A(z) = -\frac{\alpha}{z-\beta} - \gamma$. There is one pole at $z = \beta$ on the first (physical) sheet. At $z = \infty$ on the first sheet $S(z) \rightarrow -\gamma + \frac{n\hbar - \alpha}{z}$. Therefore, the Schwarz function has another pole at the point $-\bar{\gamma}$ on another sheet. All the poles are simple. According to the general arguments of Sec. 4, the number of sheets is 2, the number of branching points is 4. The genus is 1. The curve has the form

$$f(z, \bar{z}) = z^2 \bar{z}^2 + k_1 z^2 \bar{z} + \bar{k}_1 z \bar{z}^2 + k_2 z^2 + \bar{k}_2 \bar{z}^2 + k_3 z \bar{z} + k_4 z + \bar{k}_4 \bar{z} + h = 0.$$

The points at infinity and $-\bar{\gamma}$ belong to the second sheet of the algebraic covering. Summing up,

$$S(z) = \begin{cases} -\frac{\alpha}{z-\beta} & \text{as } z \rightarrow \beta_1, \\ (-\gamma + \frac{n\hbar-\alpha}{z}) & \text{as } z \rightarrow \infty_1, \\ \frac{n\hbar-\bar{\alpha}}{z+\bar{\gamma}} & \text{as } z \rightarrow -\bar{\gamma}_2, \\ (\bar{\beta} - \frac{\bar{\alpha}}{z}) & \text{as } z \rightarrow \infty_2. \end{cases}$$

where, by 1 and 2 we indicate the sheets.

Poles and residues of the Schwarz function determine all the coefficients of the curve $f(z, \bar{z}) = a(z)(\bar{z} - S^{(1)}(z))(\bar{z} - S^{(2)}(z)) = \overline{a(z)}(z - \bar{S}^{(1)}(\bar{z}))(z - \bar{S}^{(2)}(\bar{z}))$ except one. The behavior at ∞ of z, \bar{z} gives $k_1 = \gamma - \bar{\beta}$, $k_2 = -\gamma\bar{\beta}$. Hereafter we choose the origin by setting $\gamma = 0$. The equation of the curve then reads $f_n(z, \bar{z}) = 0$, where $f_n(z, \bar{z})$ is given by

$$z^2\bar{z}^2 - z^2\bar{z}\bar{\beta} - z\bar{z}^2\beta + (|\bar{\beta}|^2 + \alpha + \bar{\alpha} - n\hbar)z\bar{z} + z\bar{\beta}(n\hbar - \alpha) + \bar{z}\beta(n\hbar - \bar{\alpha}) + h_n \quad (60)$$

The free term h_n is to be determined by filling factors of the two droplets ν_1 and $\nu_2 = n - \nu_1$. A detailed analysis shows that the droplets belong to different sheets (Fig. 10). Therefore, ν_2 is negative.

A boundary of a physical droplet is given by the equation $\bar{z} = S^{(1)}(z)$ (Fig. 3). The second droplet belongs to the unphysical sheet. Its boundary is given by $\bar{z} = S^{(2)}(z)$. The explicit form of both branches is

$$S^{(1,2)} = \frac{1}{2}\bar{\beta} - \frac{\beta(n\hbar - \bar{\alpha}) + (\alpha + \bar{\alpha} - n\hbar)z \mp \sqrt{(z - z_1)(z - z_2)(z - z_3)(z - z_4)}}{2(z - \beta)z},$$

where the branching points z_i depend on h_n .

If the filling factor of the physical droplet is equal to n , the cut inside the unphysical droplet is of the order of $\sqrt{\hbar}$. Although it never vanishes, it shrinks to a double point $z_3 = z_4 = z_*$ in a semiclassical limit. The sheets meet at the double point z_* rather than along the cut: $\sqrt{(z - z_1)(z - z_2)(z - z_3)(z - z_4)} \rightarrow (z - z_*)\sqrt{(z - z_1)(z - z_2)}$. In this case, genus of the curve reduces to zero and the exterior of the physical droplet becomes an algebraic domain. This condition determines h , and also the position of the double point (Fig. 11). The double point is a saddle point for the level curves of $f(z, \bar{z})$. If all the parameters are real, the double point is stable in x -direction and unstable in y -direction. A saddle point is a signature of a virtual droplet [4].

If this solution is chosen, the exterior of the physical droplet can be mapped

to the exterior of the unit disk by the Joukowski map

$$z(w) = rw + u_0 + \frac{u}{w - a}, \quad |w| > 1, \quad |a| < 1. \quad (61)$$

The inverse map is given by the branch $w_1(z)$ (such that $w_1 \rightarrow \infty$ as $z \rightarrow \infty$) of the double valued function

$$w_{1,2}(z) = \frac{1}{2r} \left[z - u_0 + ar \pm \sqrt{(z - z_1)(z - z_2)} \right], \quad z_{1,2} = u_0 + ar \mp 2\sqrt{r(u + au_0)}.$$

The function

$$\bar{z}(w^{-1}) = rw^{-1} + \bar{u}_0 + \frac{\bar{u}}{w^{-1} - \bar{a}} \quad (62)$$

is a meromorphic function of w with two simple poles at $w = 0$ and $w = \bar{a}^{-1}$. Treated as a function of z , it covers the z -plane twice. Two branches of the Schwarz function are $S^{(1,2)}(z) = \bar{z}(w_{1,2}^{-1}(z))$. On the physical sheet, $S^{(1)}(z) = \bar{z}(w_1(z))$ is the analytic continuation of \bar{z} away from the boundary. This function is meromorphic outside the droplet. Apart from a cut between the branching points $z_{1,2}$, the sheets also meet at the double point $z_* = -\bar{\gamma} + a^{-1}re^{2i\phi}$, where $S^{(1)}(z_*) = S^{(2)}(z_*)$, $\phi = \arg(ar + \frac{u\bar{a}}{1-|a|^2})$.

Analyzing singularities of the Schwarz function, one connects parameters of the conformal map with the deformation parameters:

$$\begin{cases} \gamma = \frac{\bar{u}}{a} - \bar{u}_0, \\ n\hbar - \bar{\alpha} = r^2 - \frac{ur}{a^2}, \\ \beta = \frac{r}{a} + u_0 + \frac{u\bar{a}}{1-|a|^2} \end{cases} \quad (63)$$

$$\text{Area of the droplet} \sim n\hbar = r^2 - \frac{|u|^2}{(1-|a|^2)^2}.$$

A critical degeneration occurs when the double point merges with a branching point located inside the droplet ($z_* = z_2$) to form a triple point z_{**} . This may happen on the boundary only. At this point, the boundary has a (2, 3) cusp (Fig. 12). In local coordinates, it is $x^2 \sim y^3$. This is a critical point of the conformal map: $w'(z_{**}) = \infty$. A critical point inevitably results from the evolution at some finite critical area.

A direct way to obtain the complex curve from the conformal map is the following. First, rewrite (61) and (62) as

$$\begin{cases} z - u_0 + ar = rw + a(z + \bar{\gamma})w^{-1} \\ \bar{z} - \bar{u}_0 + \bar{a}r = rw^{-1} + \bar{a}(\bar{z} + \gamma)w, \end{cases} \quad (64)$$

and treat w and $1/w$ as independent variables. Then impose the condition $w \cdot w^{-1} = 1$. One obtains

$$\left| \det \begin{bmatrix} z - u_0 + ar & a(z + \gamma) \\ \bar{z} - \bar{u}_0 + \bar{a}r & r \end{bmatrix} \right|^2 = \left(\det \begin{bmatrix} r & a(z + \bar{\gamma}) \\ \bar{a}(\bar{z} + \gamma) & r \end{bmatrix} \right)^2.$$

This gives the equation of the curve and in particular h , in terms of u , u_0 , r , a and eventually through the deformation parameters α , β , γ and t .

The semiclassical analysis gives a guidance for the form of the recurrence relations. Let us use an ansatz for the L -operator, which resembles the conformal map (61):

$$L = r_n \hat{w} + u_n^{(0)} + (\hat{w} - a_n)^{-1} u_n,$$

so that

$$(\hat{w} - a_n)L = (\hat{w} - a_n)r_n \hat{w} + (\hat{w} - a_n)u_n^{(0)} + u_n, \quad (65)$$

$$L^\dagger(\hat{w}^{-1} - \bar{a}_n) = \hat{w}^{-1}r_n(\hat{w}^{-1} - \bar{a}_n) + \bar{u}_n^{(0)}(\hat{w}^{-1} - \bar{a}_n) + \bar{u}_n, \quad (66)$$

where \hat{w} is the shift operator $n \rightarrow n + 1$.

Now we follow the procedure of the previous section. Since the potential has only one pole, \mathcal{L}_n can be cast into 2×2 matrix form. Let us apply the lines (65, 66) to an eigenvector (c_n, c_{n+1}) of a yet unknown operator \mathcal{L}_n , and set the eigenvalue to be \tilde{z} :

$$\begin{cases} (z + r_{n-1}a_{n-1} - u_n^{(0)})c_n = r_n c_{n+1} + a_{n-1}(z + \bar{\gamma}_{n-1})c_{n-1} \\ (\tilde{z} + r_n \bar{a}_n - \bar{u}_{n+1}^{(0)})c_n = \bar{a}_{n+1}(\tilde{z} + \gamma_{n+1})c_{n+1} + r_n c_{n-1}. \end{cases} \quad (67)$$

We have defined $\bar{\gamma}_n = \frac{u_n}{a_n} - u_n^0$. The equations are compatible if c_{n-1} and c_{n+1} found through c_n differ by the shift $n \rightarrow n + 2$. We have

$$c_{n+1} = \frac{c_n}{d_n} \det \begin{vmatrix} z + r_{n-1}a_{n-1} - u_n^{(0)} & a_{n-1}(z + \bar{\gamma}_{n-1}) \\ \tilde{z} + r_n \bar{a}_n - \bar{u}_{n+1}^{(0)} & r_n \end{vmatrix} = c_n \frac{\tilde{\mathcal{D}}_n}{d_n},$$

$$c_{n-1} = \frac{c_n}{d_n} \det \begin{vmatrix} r_n & z + r_{n-1}a_{n-1} - u_n^{(0)} \\ \bar{a}_{n+1}(\tilde{z} + \gamma_{n+1}) & \tilde{z} + r_n \bar{a}_n - \bar{u}_{n+1}^{(0)} \end{vmatrix} = c_n \frac{\mathcal{D}_n}{d_n},$$

where

$$d_n = \det \begin{vmatrix} r_n & a_{n-1}(z + \bar{\gamma}_{n-1}) \\ \bar{a}_{n+1}(\bar{z} + \gamma_{n+1}) & r_n \end{vmatrix}$$

This yields the curve

$$\tilde{\mathcal{D}}_n \cdot \mathcal{D}_{n+1} = d_n d_{n+1}. \quad (68)$$

Comparing the two forms of the curve (60) and (68), we obtain the conservation laws of growth:

$$\begin{aligned}\gamma &= \gamma_n = \frac{\bar{u}_n}{\bar{a}_n} - \bar{u}_n^0, \\ \beta &= \frac{r_n}{\bar{a}_{n+1}} + u_{n+1}^{(0)} + \frac{u_{n+1}^{(0)} a_n \bar{a}_{n+1}}{1 - a_n \bar{a}_{n+1}}, \\ n\hbar - \bar{\alpha} &= r_n r_{n+1} - \frac{r_{n+1} u_{n+1}}{a_n a_{n+1}}.\end{aligned}$$

They are the quantum version of (63).

The poles of the vector potential field determine most elements of the matrix \mathcal{L}_n . We have

$$\mathcal{L}_n \underline{\chi}_n = \left(\mathbf{A}_n + \frac{\mathbf{B}_n}{z} + \frac{\mathbf{C}_n}{z - \beta} \right) \underline{\chi}_n, \quad \underline{\chi}_n = (\chi_n, \chi_{n+1})^t,$$

where \mathbf{A} , \mathbf{B} and \mathbf{C} are z -independent 2×2 matrices. Their elements are $A_{11} = \bar{\beta}$, $A_{21} = \bar{\beta} a_n$, $A_{12} = A_{22} = 0$, $B_{11} = t - \bar{\alpha}$, $B_{12} = \frac{r_{n-1} r_n}{a_{n-1}}$, $B_{21} = B_{22} = 0$, $\text{tr} \mathbf{C} = -\alpha$, $\det \mathbf{C} = 0$, $\hbar n = -C_{11} - \bar{\beta} a_n (B_{12} + C_{12})$. The undetermined matrix elements are found similarly to the case of the ellipse. We treat the recurrence relation (the first line of (67)) as a 2×2 representation of the shift operator

$$\mathcal{W}_n = \begin{pmatrix} 0 & 1 \\ -z \frac{a_n}{r_{n+1}} & \frac{z + r_n a_n - u_{n+1}^{(0)}}{r_{n+1}} \end{pmatrix}$$

and compute \mathcal{L}_n from the second line of (67). The matrix elements of \mathbf{C}_n appear to be rather cumbersome.

5.3 Genus three – hypotrochoid

The potential is $V(z) = t_3 z^3$. A general polynomial potential, including this example, has been analyzed in Ref. [9]. We briefly review it here to illustrate features of the curve with multiple poles of the Schwarz function. In this case, $A(z)$ has a double pole at infinity. The number of sheets is three. The behavior of the Schwarz function at infinity is $S(z) \sim 3t_3 z^2$ and the symmetry of the potential under $2\pi/3$ -rotation restricts the equation of the curve to the form

$$f_n(z, \bar{z}) = (z\bar{z})^2 - \frac{\bar{z}^3}{3t_3} - \frac{z^3}{3t_3} + k_n z\bar{z} + h_n = 0, \quad (69)$$

with two unknown coefficients. Since $S(z)$ has a double pole at infinity on the physical sheet, it has a branching point at infinity on the other sheets. This is the point where two unphysical sheets meet. Eq.(69) suggests that there are

9 more branching points. Therefore, genus of the curve is $g = 3$. There are four droplets, but only one belongs to the physical sheet. $2\pi/3$ rotations leave the physical droplet invariant and exchange unphysical droplets. Therefore, the filling factors of unphysical droplets must be equal. This number, together with the filling factor of the physical droplet, determine the coefficients in (69).

Let us start from the semiclassical analysis. Assume that the filling factor of the physical droplet is n . We then have an algebraic domain bounded by a hypotrochoid, Fig. 4. Six critical points sitting outside the droplet collapse two by two to three double points. The function

$$z(w) = rw + \frac{u}{w^2} \quad (70)$$

maps the exterior of the unit disk to the exterior of the hypotrochoid. The inverse function has three branches $w_i(z)$, $i = 1, 2, 3$. At infinity, the three sheets have the leading terms $w_1(z) \rightarrow z/r$, $w_{2,3}(z) \rightarrow \pm(u/z)^{1/2}$. Therefore, the inverse of the map (70) is $w_1(z)$. The branch $S(z) = \bar{z}(w_1^{-1}(z))$ is the Schwarz function. It is a meromorphic function outside the domain with one double pole at infinity, $S(z) \sim 3t_3z^2 + (n\hbar)/z$. This gives $\bar{u} = 3t_3r^2$, while the area is $n\hbar = r^2 - 2|u|^2 = r^2 - 18|t_3|^2r^4$. The coefficients of the equation of the curve are determined by

$$k = \frac{(1 - 9|t_3|^2r^2)(1 + 18|t_3|^2r^2)}{9|t_3|^2}, \quad h = -\frac{r^2(1 - 9|t_3|^2r^2)^3}{9|t_3|^2}. \quad (71)$$

Four remaining branching points are $z = \infty$ and three points solving $dz = (r - 2uw^{-3})dw = 0$, at $w_*^3 = 2u/r$. They are situated inside the droplet. Three double points solve $S^{(i)}(z) = S^{(j)}(z)$. They are outside the droplet:

$$z_*^3 = \frac{(r^2 - |u|^2)^3}{|u|^2\bar{u}}.$$

At a critical degeneration the double points merge on the boundary to the branching point inside the droplet, $z_* = z(w_*)$, $|w_*| = 1$ (Fig. 7).

Quantum analysis starts from recurrence relations guided by the classical case. Eqs. (20, 18) read

$$z\psi_n = r_n\psi_{n+1} + u_n\psi_{n-2}, \quad (L^\dagger\psi)_n = r_{n-1}\psi_{n-1} + \bar{u}_{n+2}\psi_{n+2}. \quad (72)$$

Acting on the eigenvector of \mathcal{L}_n , we get

$$\begin{cases} zc_n = r_nc_{n+1} + u_nc_{n-2} \\ \tilde{z}c_n = r_{n-1}c_{n-1} + \bar{u}_{n+2}c_{n+2}. \end{cases}$$

Writing the first equation for $n \rightarrow n \pm 1$, we express c_{n+2} and c_{n-1} through c_n and c_{n+1} to obtain

$$\tilde{z}c_n = z \frac{\bar{u}_{n+2}}{r_{n+1}} c_{n+1} + \frac{1}{r_{n+1}} (r_{n-1} r_{n+1} - u_{n+1} \bar{u}_{n+2}) c_{n-1},$$

$$zc_n = \left(r_n - \frac{u_n \bar{u}_{n+1}}{r_{n-2}} \right) c_{n+1} + \bar{z} \frac{u_n}{r_{n-2}} c_{n-1}.$$

Equations are compatible if \tilde{z} belongs to the curve

$$\det \begin{vmatrix} \left(r_{n+1} - \frac{u_{n+1} \bar{u}_{n+2}}{r_{n-1}} \right) z & \\ \frac{z \bar{u}_{n+3}}{r_{n+2}} & \tilde{z} \end{vmatrix} \cdot \det \begin{vmatrix} z & \frac{\tilde{z} u_n}{r_{n-2}} \\ \tilde{z} & \left(r_{n-1} - \frac{u_{n+1} \bar{u}_{n+2}}{r_{n+1}} \right) \end{vmatrix} = d_n d_{n+1},$$

where

$$d_n = \det \begin{vmatrix} \left(r_n - \frac{u_n \bar{u}_{n+1}}{r_{n-2}} \right) & \frac{\tilde{z} u_n}{r_{n-2}} \\ \frac{z \bar{u}_{n+2}}{r_{n+1}} & \left(r_{n-1} - \frac{u_{n+1} \bar{u}_{n+2}}{r_{n+1}} \right) \end{vmatrix}.$$

Comparing with (69), we find the quantum version of (71):

$$k_n = r_n^2 \left[1 - 9|t_3|^2 (r_{n-1}^2 + r_{n+1}^2) + \frac{1}{9|t_3|^2 r_n^2} \right],$$

$$h_n = -\frac{r_n^2}{9|t_3|^2} (1 - 9|t_3|^2 r_{n-1}^2) (1 - 9|t_3|^2 r_n^2) (1 - 9|t_3|^2 r_{n+1}^2),$$

where we used the conservation law and a quantum analog of the area formula

$$3t_3 = \frac{\bar{u}_{n+1}}{r_{n-1} r_{n+1}}, \quad r_n^2 - (|u_{n+2}|^2 + |u_{n+1}|^2) = \hbar n.$$

Together, these equations give a closed equation for r_n^2 ,

$$r_n^2 (1 - |3t_3|^2 (r_{n+1}^2 + r_{n-1}^2)) = \hbar n,$$

which is a discrete analog of the Painlevé I equation.

The matrix form of L^\dagger can be obtained in a similar manner. It is a 3×3 matrix acting on the 3-vector $(\chi_n, \chi_{n+1}, \chi_{n+2})^t$. Its analytic structure is

$$\mathcal{L}_n = \mathbf{A}_n + z \mathbf{B}_n + z^2 \mathbf{C}_n,$$

and the matrices \mathbf{A} , \mathbf{B} , \mathbf{C} are

$$\mathbf{A}_n = \begin{pmatrix} 0 & 0 & \frac{r_n}{r_{n-1}} (3\bar{t}_3)^{-1} (1 - |3t_3|^2 r_{n-1}^2) \\ r_{n-1} (1 - |3t_3|^2 r_n^2) & 0 & 0 \\ 0 & r_n (1 - |3t_3|^2 r_{n+1}^2) & 0 \end{pmatrix},$$

$$\mathbf{B}_n = \begin{pmatrix} 0 & \frac{1}{r_{n-1}}(3\bar{t}_3)^{-1} & 0 \\ 0 & 0 & 3t_3 r_n \\ -|3t_3|^2 r_n r_{n-1} & 0 & 0 \end{pmatrix}, \quad \mathbf{C}_n = \begin{pmatrix} 0 & 0 & 0 \\ 0 & 0 & 0 \\ 0 & 0 & 3t_3 \end{pmatrix}.$$

6 Semiclassical wave function

In the semiclassical limit, $\hbar \rightarrow 0$, while $t = \hbar N$, $t^{(\alpha)} = \hbar \nu_\alpha$, and the potential $V(z)$ are kept fixed. The quantum curve and evolution equations go to their semiclassical counterparts. Also, the semiclassical wave functions are written through the objects of the semiclassical theory, i.e., through differentials on the semiclassical curve.

A technical difficulty is that wave functions with close indices, say ψ_n and ψ_{n+1} , are not necessarily close to each other as $n \rightarrow \infty$. Choosing a sequence of states which has a semiclassical limit is sensitive to the potential, and reflects the configuration of semiclassical droplets. This problem does not arise in the case of a single droplet in the algebraic case, where states with close numbers are close. As we discussed above, this case corresponds to degenerate Riemann surfaces. Hereafter, we assume that states with close n 's are close, and proceed to the semiclassical limit. The result obtained for this case can be generalized to any smooth Riemann surface.

First, we rewrite the L operator (20) in a more symmetric form $L = \hat{w}^{-1/2} r \hat{w}^{1/2} + \sum \hat{w}^{-k/2} u^{(k)} \hat{w}^{-k/2}$, by redefining r and $u^{(k)}$. Then we search for a semiclassical expansion

$$\psi(z) \sim e^{\frac{1}{\hbar} \mathcal{A}_0(z) + \mathcal{A}_1(z) + \dots}$$

(in what follows, we suppress the index n).

In the first two leading orders, the L -operator (20) reads

$$L \longrightarrow z(w) + \frac{\hbar}{2} \{w \partial_w z(w), \partial_t\} \mathcal{A}_1 + \dots,$$

where $\log w = \partial_t \mathcal{A}_0$ and $\{, \}$ means anticommutator. The function

$$z(w) = rw + \sum_{k \geq 0} u^{(k)} w^{-k} \quad (73)$$

is obtained by replacing the shift operator by its classical value $\hat{w} \rightarrow w$.

The recurrence relation $L\psi(z) = z\psi(z)$ in two leading orders reads

$$z(w) = z, \quad \partial_t \mathcal{A}_1 = -\frac{1}{2} \frac{\partial_t \partial_w z(w)}{\partial_w z(w)}, \quad \log w = \partial_t \mathcal{A}_0.$$

It gives

$$\mathcal{A}_1(z) = \frac{1}{2} \log w'(z), \quad (74)$$

where $w(z)$ is a multivalued function inverse to (73).

In the leading orders, (18) reads

$$\hbar \partial_z \psi(z) = \left(-\frac{\bar{z}}{2} + \bar{z}(w^{-1}) + \frac{\hbar}{2} \{w \partial_w \bar{z}(w^{-1}), \partial_t\} + \mathcal{A}_1 + \dots \right) \psi(z). \quad (75)$$

The function $\bar{z}(w^{-1})$ is the Schwarz reflection of $z(w)$ with respect to the contour whose exterior is mapped to the exterior of the unit disk by the function $w(z)$. This map is discussed in Sec. 4.1.3. The contour is the boundary of a semiclassical droplet. We observe that in the simplest semiclassical limit the conformal map and its Schwarz reflection are limits of the L and L^\dagger operators of Sec. 2. The complex curve in the semiclassical limit is given by $f(z, \bar{z}) = a(z) \prod (\bar{z} - \bar{z}(w^{-1}(z)))$, where the product is taken over all possible branches of the multivalued function $w(z)$.

Introducing the Schwarz function $S(z) = \bar{z}(w^{-1}(z))$, as in (49), we obtain

$$\mathcal{A}_0 = -\frac{|z|^2}{2} + \Omega(z),$$

where $\Omega(z) = \int_{\xi_0}^z d\Omega$ is the primitive function of the generating differential introduced in Sec. 4.2. The point ξ_0 is such that $\log w(\xi_0) = 0$. It is a boundary point. The integral goes along the physical sheet.

Summing up, we obtain the result:

$$\psi(z) \simeq (2\pi^3 \hbar)^{-1/4} \sqrt{w'(z)} e^{\frac{1}{\hbar}(-\frac{1}{2}|z|^2 + \Omega(z))}. \quad (76)$$

Formula (76) was reported in [2]. A similar formula for the two-matrix model was obtained in [33]. Being applied to the Hermite or Laguerre polynomials (see example in Sec. 5.1), the formula gives the asymptotical behaviour found by Tricomi in 1941 [34].

The overall numerical factor can be fixed either by comparison with asymptotics of biorthogonal polynomials for the Ginibre ensemble, or through normalization of the semiclassical wave function. The latter is described below.

An extension of this formula to the case of a general complex curve and multiple droplets is straightforward. The function $\Omega(z)$ should be again understood as an integral of the generating differential $d\Omega$. The integration path starts at a point on the boundary of some “reference” droplet and ends at the point z . The correction factor, $w'(z)$ in (76), is replaced by the meromorphic Abelian

differential of the third kind $W^{(\infty, \infty)}(z)$, introduced in Sec. 4.2. As a result, we obtain:

$$\psi(z)\sqrt{dz} \sim \sqrt{W^{(\infty, \infty)}(z)} e^{-\frac{1}{\hbar} \left(\frac{|z|^2}{2} - \int_{\xi_0}^z S(z) dz \right)}. \quad (77)$$

By virtue of (40), monodromies of this wave function around droplets are $e^{2\pi i \nu_\alpha}$, where ν_α are filling factors.

The asymptotical representation (77) fails around cuts or double points. It is valid only around boundaries of physical droplets and only if the distance between boundary of a physical droplet and a cut or a double point is much larger than $\sqrt{\hbar}$. In other words, it is valid for smooth non-critical curves. The semiclassical asymptotics of the wave function in the whole plane is far beyond the scope of this paper.

The following properties of \mathcal{A}_0 visualize the result.

- (i) The real part of \mathcal{A}_0 is constant along boundary of any droplet (see Sec. 4.2), generally different for different droplets

$$2\mathcal{R}e\mathcal{A}_0(z) = \phi_\alpha, \quad z \in \partial D_\alpha.$$

- (ii) Derivatives ∂_z and $\partial_{\bar{z}}$ of $\mathcal{R}e\mathcal{A}_0$ vanish on the boundary:

$$\partial_z \mathcal{R}e\mathcal{A}_0(z) = \partial_{\bar{z}} \mathcal{R}e\mathcal{A}_0(z) = 0, \quad z \in \partial D.$$

This is the condition for semiclassical extrema (41).

- (iii) In the leading order, the change of $\mathcal{R}e\mathcal{A}_0$ under small deviations along the normal direction away from the boundary to both exterior and interior does not depend on the point of the boundary:

$$\partial_n^2 \mathcal{R}e\mathcal{A}_0(z) = -2.$$

- (iv) The higher order expansion away from the boundary depends of the curvature of the boundary $k(z)$, $z \in \partial D_\alpha$:

$$\mathcal{R}e\mathcal{A}_0(z + \delta n) = \phi_\alpha - (\delta n)^2 + \frac{1}{3}k(z)(\delta n)^3 - \frac{1}{4}k^2(z)(\delta n)^4 + \dots, \quad (78)$$

where δn is a normal deviation from the boundary directed outward. This expansion fails at very curved parts of the contour, where $k(z) \sim \hbar^{-1/2}$.

Altogether, these properties mean that the wave function peaks at the boundary of a physical droplet and decays as Gaussian at the rate $\sqrt{\hbar}$ (see Fig. 6):

$$|\psi(z + \delta n)|^2 \sim e^{\frac{\phi_\alpha}{\hbar}} e^{-\frac{2}{\hbar}(\delta n)^2}, \quad z \in \partial D_\alpha. \quad (79)$$

The amplitude of the wave function may be different on different boundaries.

Since the wave function is localized on the boundary, one can integrate in the normal direction. In the case of one droplet, we have

$$\int |\psi(z)|^2 d(\delta n) = \frac{1}{2\pi} \partial_n \log |w(z)| = \frac{1}{2\pi} |w'(z)|, \quad z \in \partial D \quad (80)$$

(here ∂_n is the normal derivative). Further integration along the boundary is consistent with the normalization $\int |\psi_N(z)|^2 d^2z = 1$. This can be used to determine the constant in (76).

According to the arguments of Sec. 1.6, Eq. (80) can be interpreted as a rate of growth.

Note that Eq. (74) and the next to leading order of (75) give the relation

$$w(\partial_w z \partial_t \bar{z} - \partial_t z \partial_w \bar{z}) = 2, \quad (81)$$

where one differentiates at a fixed w . This relation represents evolution of the growing domain as a time-dependent conformal map. The area of the domain grows linearly with time, while its harmonic moments stay fixed. This type of classical growth is equivalent to the Laplacian growth. Relation (81) has been known in the literature for a long time [38]. It is a classical limit of Eq. (21).

7 Appendix. Laplacian growth

Laplacian growth refers to growth of a planar domain, whose boundary propagates with a velocity proportional to the gradient of a harmonic field. The Hele-Shaw problem is a typical example (see [31] for a review). The experimental set-up consists (Fig. 13) of two parallel and horizontal glass plates, separated by a small distance along the vertical direction, called *the gap*, b . The gap is small enough compared to typical intermolecular distances in fluids, so that the system can be considered two-dimensional.

Initially, the space between the plates is filled with fluid 2, of large viscosity (typical examples are silicon oil or liquid crystals). Through a small opening in the middle of the upper glass plate, fluid 1, of much lower viscosity (such as air), is inserted into the system, at a constant rate. Both fluids are incompressible and immiscible, so fluid 2 must be evacuated from the system at the same rate as fluid 1 is being introduced. This is done somewhere at the edge of the glass plates.

Given that the fluids are incompressible and immiscible, the dynamics of the system is reduced to that of the interface between them. Depending on the relevant parameters of the experiment (the coefficients of viscosity, $\mu_{1,2}$ of the

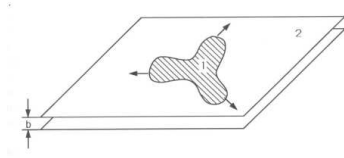


Fig. 13. The Hele-Shaw setup.

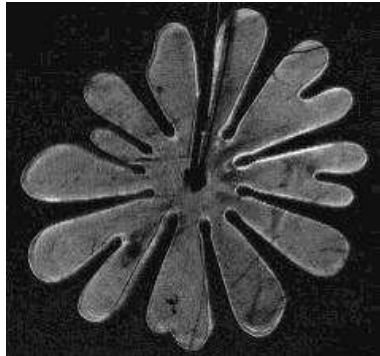


Fig. 14. Laminar Hele-Shaw dynamics.

fluids, the coefficient of surface tension σ , the gap b and the pumping rate Q), the interface dynamics will exhibit very different behaviors. At low pumping rates Q , for given σ , the interface will remain smooth at all times, regardless of how much fluid is being inserted (Fig. 14). However, at high Q (or equivalently, at very low σ), the boundary will develop the so-called *fingering instability*, where certain regions grow in the shape of fingers, whose tips split and form secondary fingers, etc. Real experiments (Fig. 5) show that in this regime, the interface seems to evolve into a self-similar, fractal structure.

Under the assumption that the system is two dimensional, the equations governing the dynamics of the interface lead to Darcy's Law: the velocity field \vec{v}_i and pressure p_i in fluid i are related as:

$$\vec{v}_i = -\frac{b^2}{12\mu_i}\vec{\nabla}p_i, \quad (82)$$

and therefore the continuity equation across the interface leads to

$$\vec{v} \cdot \vec{n} = -\frac{b^2}{12\mu_1}\vec{n} \cdot \vec{\nabla}p_1 = -\frac{b^2}{12\mu_2}\vec{n} \cdot \vec{\nabla}p_2, \quad (83)$$

where \vec{n} is the unit vector normal to the interface at a given point.

In each fluid, the pressure field is supposed to solve the Laplace equation,

$$\Delta p_i = 0, \quad (84)$$

with appropriate boundary conditions. For instance, since fluid 2 is drained

from the system somewhere away from the origin, fluid 2 has a sink at infinity, which leads to the condition

$$p_2(z) \rightarrow -\log |z|, \quad z \rightarrow \infty. \quad (85)$$

The coefficient of surface tension enters the problem through the Laplace formula relating the pressure jump across the boundary and the local curvature $\kappa(z)$:

$$p_2(z) - p_1(z) = \sigma \kappa(z). \quad (86)$$

The first simplification of the problem consists in setting the viscosity of fluid 1 to zero, $\mu_1 = 0$. The continuity condition then implies $p_1 = \text{constant}$, and we may therefore choose $p_1 = 0$ (a redefinition of p_2).

The second important simplification is neglecting the effect of surface tension. This assumption has important physical meaning, since the resulting problem should necessarily lead to turbulent dynamics. Mathematically, the two assumptions lead to the following reformulation of the problem:

$$\Delta p = 0 \text{ on } D_-, \quad p = 0, \quad V_n \sim \partial_n p \text{ on } \Gamma, \quad p(z) \xrightarrow{z \rightarrow \infty} -\log |z|, \quad (87)$$

where V_n is the normal component of the velocity, D_- is the domain occupied by fluid 2, and Γ is the boundary between fluids. Under these assumptions, in order to describe the interface dynamics, we must solve an exterior Dirichlet problem for the pressure field.

Acknowledgments

We are indebted to A. Kapaev, V. Kazakov, I. Krichever, I. Kostov, A. Marshakov and M. Mineev-Weinstein for useful discussions, interest in the subject and help. P.W. and R.T. were supported by the NSF MRSEC Program under DMR-0213745, NSF DMR-0220198 and by the Humboldt foundation. A.Z. and P.W. acknowledge support by the LDRD project 20020006ER “Unstable Fluid/Fluid Interfaces” at Los Alamos National Laboratory and M. Mineev-Weinstein for the hospitality in Los Alamos. A.Z. was also supported in part by RFBR grant 03-02-17373 and by the grant for support of scientific schools NSh-1999.2003.2. P.W. is grateful to K.B. Efetov for the hospitality in Ruhr-Universitaet Bochum and to A.Cappelli for the hospitality in the University of Florence, where this work was completed. We are grateful to Harry Swinney for permitting us to use Fig. 5 from [16].

References

- [1] Mineev-Weinstein, M., Wiegmann, P.B., & Zabrodin, A., 2000, Phys. Rev. Lett. **84**, 5106.
- [2] Agam, O., Bettelheim, E., Wiegmann, P.B., & Zabrodin, A., Viscous Fingering and a Shape of an Electronic Droplet in a Quantum Hall Regime, 2002, Phys. Rev. Lett. **88**, 236802.
- [3] Krichever, I., Mineev-Weinstein, M., Wiegmann, P.B., & Zabrodin, A., Laplacian growth and Whitham Equations of Soliton Theory, 2003, nlin.SI/0311005.
- [4] Dijgraaf, R., & Vafa, C., $\mathcal{N} = 1$ Supersymmetry, Deconstruction and Bosonic Gauge Theory, 2003, hep-th/0302011, A Perturbative Window into Non-Perturbative Physics, 2002, hep-th/0208048, Matrix Models, Topological Strings and Supersymmetric Gauge Theories, 2002, hep-th/0206255, On Geometry and Matrix Models, 2002, hep-th/0207106.
- [5] Bertola, M., Eynard, B. & Harnad, J., Partition functions for Matrix Models and Isomonodromic Tau Functions, 2002, nlin/0204054.
- [6] Kapaev, A., Riemann-Hilbert problem for bi-orthogonal polynomials, 2003, J. Phys. A **36**, 4629-4640.
- [7] Di Francesco, P., Ginsparg, P., & Zinn-Justin, J., 2-D Gravity and Random Matrices, 1995, Phys. Rept. 254, 1-133.
- [8] Fokas, A.S., Its, A.R., & Kitaev, A., The isomonodromy approach to the matrix models in 2-D gravity, 1992, Comm. Math. Phys. 147, 395-430.
- [9] Kazakov, V.A., & Marshakov, A., Complex Curve of the Two Matrix Model and its Tau-function, 2003, J. Phys. A **36**, 3107-3136.
- [10] Chekhov, L., & Mironov, A., Matrix Models vs. Seiberg-Witten/Whitham theories, 2002, hep-th/0209085.
- [11] David, F., Non-Perturbative Effects in Matrix Models and Vacua of Two Dimensional Gravity, 1993, Phys.Lett. B302, 403-410; hep-th/9212106; David, F., Bonnet, G., & Eynard, B., Breakdown of universality in multi-cut matrix models, 2000, J.Phys. A33, 6739.
- [12] Chau, Ling-Lie, & Zaboronsky, O., On the structure of Normal Matrix Model, 1998, Commun. Math. Phys. 196, 203-247, hep-th/9711091.
- [13] Mehta, M.L., Random Matrices, 1991, Academic Press, New York.
- [14] Wiegmann, P.B., & Zabrodin, A., Large Scale Correlations in Normal and General Non-Hermitian Matrix Ensembles, 2003, J. Phys. A, **36**, 3411-3424.
- [15] Ginibre, J., Statistical Ensembles of Complex Quaternion and Real Matrices, 1965, Journal of Math. Phys. **6** (3), 440. Girko, V.L., Elliptic Law, 1986, Theory of Probability and Its Applications, 30, (4), 677-690.

- [16] Sharon, E., Moore, M.G., McCormick, W.D., & Swinney, H.L., Coarsening of Fractal Viscous Fingering Patterns, 2003, Phys. Rev. Lett., 91, 205504.
- [17] Altshuler, B.L., & Simons, B.D., Universalities: from Anderson Localization to Quantum Chaos, in: Mesoscopic Quantum Physics, 1994, Les Houches 1994, eds. Akkermans, E., Montambaux, G., Pichard, J-L., & Zinn-Justin, J.
- [18] Aratyn, H., Integrable Lax Hierarchies, their Symmetry Reductions and Multi-Matrix Models, 1995, hep-th/9503211.
- [19] Bertola, M., Eynard B., & Harnad, J., Duality of spectral curves arising in two-matrix models, 2001, nlin/0112006.
- [20] Bertola, M., Eynard, B., & Harnad, J., Differential systems for biorthogonal polynomials appearing in 2-matrix models and the associated Riemann-Hilbert problem, 2002, nlin/0208002.
- [21] Krichever, I.M., Funkt. Analiz i ego Pril., 1995, **29/2**, 1-8.
- [22] Wasow, W., Asymptotic Expansions for Ordinary Differential Equations, 1965, John Wiley & Sons, New York.
- [23] Dubrovin, B.A., Krichever, I.M., & Novikov, S.P., Topological and algebraic geometry methods in contemporary mathematical physics II, 1982, Soviet Scient. Reviews, Math. Phys. Reviews 3 1-150; Krichever, I.M., Integration of nonlinear equations by the method of algebraic geometry, 1977, Funct. Anal. Appl., **11**, 12-26.
- [24] Ahlfors, L.V., Complex Analysis, an Introduction to the Theory of Analytic Functions of One Complex Variable, 1953, McGraw-Hill, New York.
- [25] Cohn, H., Conformal Mapping on Riemann Surfaces, 1967, Dover, New York.
- [26] Schiffer, M., & Spencer, D.C., Functionals of finite Riemann surfaces, 1954, Princeton University Press.
- [27] Jimbo, M., Miwa, T., & Ueno, K., Monodromy preserving deformations of linear ordinary differential equations with rational coefficients I, 1981, Physica D, **2**, 306-52; Jimbo, M., & Miwa, T., Monodromy preserving deformation of linear ordinary differential equations with rational coefficients II, 1981, Physica D, **2**, 407-48; Flaschka, H., & Newell, A.C., Monodromy- and spectrum-preserving deformations, 1980, Commun. Math. Phys., **76**, 65-116.
- [28] Takasaki, K., Dual Isomonodromic Problems and Whitham Equations, 1998, Lett. Math. Phys. **43** 123-135.
- [29] Aharonov, D., & Shapiro, H., 1976, J. Anal. Math., **30**, 39-73; Shapiro, H., The Schwarz function and its generalization to higher dimensions, 1992, University of Arkansas Lecture Notes in the Mathematical Sciences, Volume 9, Summers W.H., Editor, John Wiley & Sons.
- [30] Kostov, I.K., Conformal field theory techniques in random matrix models, 1999, arXiv:hep-th/9907060.

- [31] Bensimon, D., Kadanoff, L.P., Liang, S., Shraiman, B.I., & Tang, C., 1986, *Rev. Mod. Phys.* **58**, 977.
- [32] Kostov, I.K., Krichever, I., Mineev-Weinstein, M., Wiegmann, P.B., & Zabrodin, A., τ -Function for Analytic Curves, in: *Random matrices and their applications*, 2000, MSRI publications, vol. 40, 285, Cambridge University Press.
- [33] Eynard, B., *Eigenvalue Distribution of Large Random Matrices, from One Matrix to Several Coupled Matrices*, 1997, cond-mat/9707005.
- [34] Bateman, H., & Erdelyi, A., *Higher transcendental functions*, 1953, v. 2, McGraw-Hill.
- [35] Marshakov, A., Mironov, A., & Morozov, A., Generalized matrix models as conformal field theories: Discrete case, 1991, *Phys. Lett. B*, **265**, 99; Kharchev, S., Marshakov, A., Mironov, A., Morozov, A., & Pakuliak, S., Conformal matrix models as an alternative to conventional multimatrix models, 1993, *Nucl. Phys. B* **404**, 717, [arXiv:hep-th/9208044].
- [36] Ueno, K., & Takasaki, K., 1984, *Adv. Stud. Pure Math.*, **4**, 1.
- [37] Whitham, J.B., *Linear and nonlinear waves*, Wiley-Interscience, 1974, New York; Flaschka, H., Forest, M.G., & McLaughlin, D.W., Multiphase averaging and the inverse spectral solution of the Korteweg-de Vries equation, 1980, *Comm. Pure Appl. Math.*, **33**, 739-84; Krichever, I.M., Method of averaging for two-dimensional “integrable” equations, 1988, *Funct. Anal. Appl.*, **22**, 200-213.
- [38] Galin, L.A., 1945, *Dokl. Akad. Nauk SSSR*, **47**, 250-253; Polubarinova-Kochina, P.Ya., 1945, *Dokl. Akad. Nauk SSSR*, **47**, 254-257; Kufarev, P.P., 1947, *Dokl. Akad. Nauk SSSR* **57**, 335-348.
- [39] Akemann, G., The Solution of a Chiral Random Matrix Model with Complex Eigenvalues, 2002, *J. Phys.* **A36**, 3363.
- [40] Wiegmann, P.B., & Zabrodin, A., Conformal maps and dispersionless integrable hierarchies, 2000, *Commun.Math.Phys.* **213**, 523-538; Marshakov, A., Wiegmann, P.B., & Zabrodin, A., Integrable Structure of the Dirichlet Boundary Problem in Two Dimensions, 2002, *Commun. Math. Phys.* **227**, 131-153.
- [41] Krichever, I., Marshakov, A., & Zabrodin, A., Integrable Structure of the Dirichlet Boundary Problem in Multiply-Connected Domains, 2003, hep-th/0309010.